LATE CENOZOIC SEISMIC STRATIGRAPHY OF THE MOHICAN CHANNEL AREA, SCOTIAN SLOPE

By

Maureen C. White

Submitted in Partial Fulfillment of the Requirements
for the Degree of Bachelor of Science, Honours

Department of Earth Sciences
Dalhousie University
Halifax, Nova Scotia
March 2005

Dalhousie University

Department of Earth Sciences
Halifax, Nova Scotia
Canada B3H 3J5
(902) 494-2358
FAX (902) 494-6889

DATE: April 22, 2005

AUTHOR: Maureen C. White

TITLE: Late Cenozoic Seismic Stratigraphy of the Manican Channel Area, Scotian Slope

Degree: B.Sc. Convocation: May 24/05 Year: 2005

Permission is herewith granted to Dalhousie University to circulate and to have copied for non-commercial purposes, at its discretion, the above title upon the request of individuals or institutions.

ABSTRACT

Nova Scotia and its continental margin have endured numerous shelf-crossing glaciations and eustatic sea level lowstands during the Cenozoic. As a result, the sedimentary sequence is not well preserved and therefore the geologic record is not well understood. In the deep water of the Scotian Slope, on the other hand, there is an opportunity to study the preserved sedimentary sequence. The objective of this study is to apply high-resolution, two-dimensional seismic surveying on the Scotian Slope to understand Cenozoic depositional environments and their associated sedimentation processes, in relation to glacial and non glacial epochs, and sea level change. The Mohican Channel area is an ideal site for this study because it contains a comprehensive record of the Plio-Pleistocene sedimentary sequence.

Within the study area, an experimental seismic system known as the digital deep-towed hydrophone (DDH) was tested in an effort to improve seismic resolution and therefore interpretation. The DDH consists of a source towed at the sea surface and a receiver towed at depth. This unconventional geometry is predicted to result in greatly improved vertical and horizontal resolution compared with its conventional seismic equivalent. Trial seismic lines have proven to significantly increase near surface resolution; however, imaging at depth within the section is lost in comparison to conventional surface seismic reflection profiles. For the objectives in this study, conventional seismic profiles, with greater imaging depths, were the most useful. These profiles allowed definition of five seismic facies and regional correlation of six seismic horizons. These are broadly grouped into two stratigaphic units which correspond to pre-glacial and glacial/interglacial periods.

Prior to the onset of glacial influence, at approximately 0.45 Ma, major sedimentation processes included hemipelagic sedimentation, unconfined low density turbidity current deposition, and mass transport deposition, as interpreted from the seismic data. Throughout the mid-Late Pleistocene glacial periods, deposition was dominated by turbidity currents derived from high volumes of glacial discharge. Interglacial stages were dominated by hemipelagic sedimentation. The Mohican Channel incises the entire Pleistocene section suggesting it is at least late Pleistocene in age. The channel is interpreted as a major glacial outwash conduit that was active during the last glacial maximum and possibly during each preceding shelf-crossing glaciation.

Thickness of the Pliocene stratigraphy does not vary over the slope, indicating that pre-glacial deposition was uniform over the study area. In comparison, mid-late Pleistocene stratigraphy thins both downslope and westward towards the Mohican Channel, indicating preferential deposition on the upper slope from a northwestern sediment source during glacial periods. Approximate sedimentation rates show that deposition during glacial influence was at least double that of non-glacial periods, indicating that glaciation plays an important role in the evolution of deep water sediments on the Scotian Slope.

TABLE OF CONTENTS

LIST OF FIGURES

LIST OF TABLES

ACKNOWLEDGEMENTS

My deepest thanks go out to my excellent supervisory committee, "The Triad". Dr. Dave Mosher of the GSC (Atlantic) went through great efforts to hire me for a work term and offered me the rewarding experience of participating in a research cruise onboard the CCGS Hudson this past summer. Without his guidance this thesis would not have been possible. Dr. Patrick Ryall of Dalhousie University has been a supportive advisor to me since my first year here in Earth Sciences and his encouragement throughout my thesis is most appreciated. Dr. Grant Wach has always managed to find time to answer my questions. His dedication to students like me has been a constant source of motivation for me throughout this project.

I would also like to extend a big thanks to Dr. David Piper of the GSC (Atlantic), whose insight into my project has been most welcome and to Calvin Campbell, who has patiently put up with my frequent pestering over the past year.

My family and friends have rocked throughout this process; their support has been such a blessing to me and they deserve a special thank-you. I will be forever grateful to my fellow classmates here at Dal who have helped me balance work with some much needed fun! May I be fortunate enough to have such a great group of people to work with in the future. I wish them all the best.

CHAPTER 1
INTRODUCTION

1.0 Introduction

In recent decades, innovation and advancement in technology have enabled the study of deep-water sedimentation processes. Seismic reflection surveying, multibeam hydrography, and core sampling, to name a few, have provided valuable data to further the understanding of the past and present geological processes in the offshore environment.

Increased industrial activity offshore Nova Scotia has necessitated the study of recent and surficial marine geology on the continental margin in an effort to assess the risk of geological hazards. Hydrocarbon development, deep-water pipeline infrastructures and cable systems offshore Nova Scotia are all industries in which the mitigation of this risk is important. Knowledge of the history of mass wasting and the regional geological framework of the Scotian Slope are integral to planning today's offshore development.

1.1 Objectives

The objective of this study is to generate a late Cenozoic geological framework of the Mohican Channel area on the central Scotian Slope through interpretation of high-resolution 2D seismic data. These high-resolution data encompass the shallow geology; approximately 500 – 800 m beneath the seafloor, which represents sediments of the Late Pliocene to Recent time. Primarily, this investigation is aimed at understanding

sedimentation processes, the relative timing of these processes, their implications for late Cenozoic conditions and the critical link to Quaternary, shelf-crossing glaciations.

In interpreting the seismic stratigraphy, this thesis examines a novel seismic acquisition technique and its role in seismic interpretation through comparison with conventional 2D reflection surveying. The digital deep-towed hydrophone (DDH) was designed by the Geological Survey of Canada (Atlantic) and tested within the study area. In theory, this system should increase the resolution of seismic data, improving interpretation.

1.2 Physiography

It is necessary to define several terms which will be used within the study to describe the physiography of the continental margin. The continental shelf, slope and rise are the primary components of the Atlantic margin. Figure 1.1 illustrates the relationship of these elements.

The continental shelf is the part of the margin that extends from coastal land to the continental slope. Typically, it reaches water depths of roughly 200 m at a gradient less than 0.1° before breaking at the higher gradient of the slope (Emery & Uchupi, 1984). Along the Scotian Margin, the shelf breaks at approximate depths of 200 m below sea level (mbsl).

The continental slope is classified as the bathymetric transition from the continental shelf break to the continental rise or locally to the abyssal plain (Emery & Uchupi, 1984). It is the region of the continental margin with the greatest slope angle and

offshore Nova Scotia it has a mean gradient of 3°, extending to water depths of 2000 – 2500 mbsl (Piper, 2001).

The continental rise is the physiographic transition from continental slope to abyssal plain. The continental rise begins where the high gradient of the slope tapers into a more gradual angle of approximately 1° (Kidston et al., 2002). This boundary is very subtle in comparison to the continental shelf break.

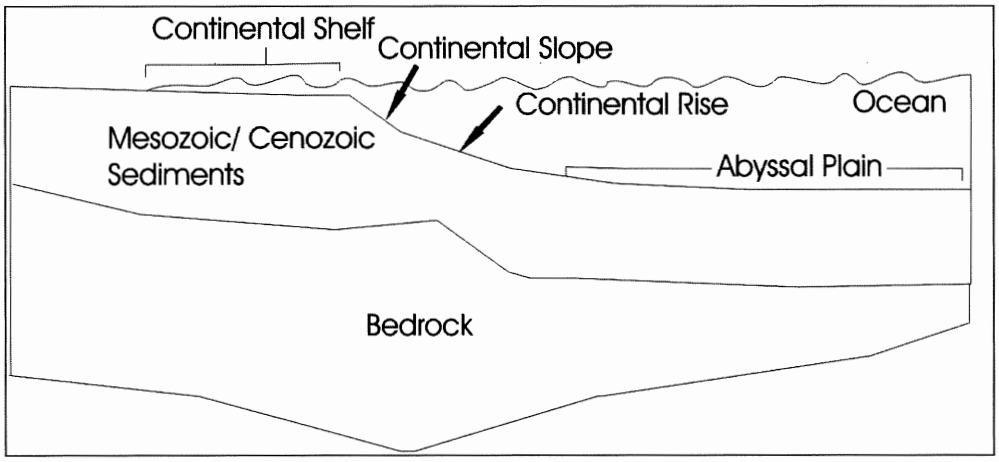

Fig. 1.1 – Schematic diagram of the physiography of the continental margin.

1.3 Study Area

The Scotian Slope extends 1000 km from the Northeast Channel in the southwest to the Laurentian Channel in the northeast, offshore Nova Scotia, and is aligned approximately parallel to the coastline (Campbell et al., 2004). The slope is subdivided into three broad geographic areas; the eastern, central and western slopes. The eastern Scotian Slope displays high topographic relief with widespread canyon dissection and an average regional gradient between 3 – 4°. The central Scotian Slope is smooth in comparison to the surfaces to the east and west, and although canyons are absent, small

gullies and escarpments are common. The gradient of the central slope ranges between 2 - 4° (Mosher et al, 2004). Finally, the western Scotian Slope is significantly eroded with a variable slope angle from gradients of 3 – 4° upslope, to gradients of 1.5 - 3° on the mid and lower slope (Campbell et al., 2004).

The study area lies on the central Scotian Slope, approximately 300 km off the coast of Nova Scotia (Figure 1.2). It encompasses an area of approximately 3000 km^2 between 42° 56'N and 42° 26'N latitudes and 62° 32'W and 61° 39'W longitudes. Water depth varies from 200 - 2500 mbsl with an average gradient of 3°. It is bounded to the east by the Acadia Valley system. The Mohican Channel, a major morphological feature bounds the study area to the west. Surficially, the region is smooth in comparison to the highly canyoned slope to the east (Mosher et al., 2004).

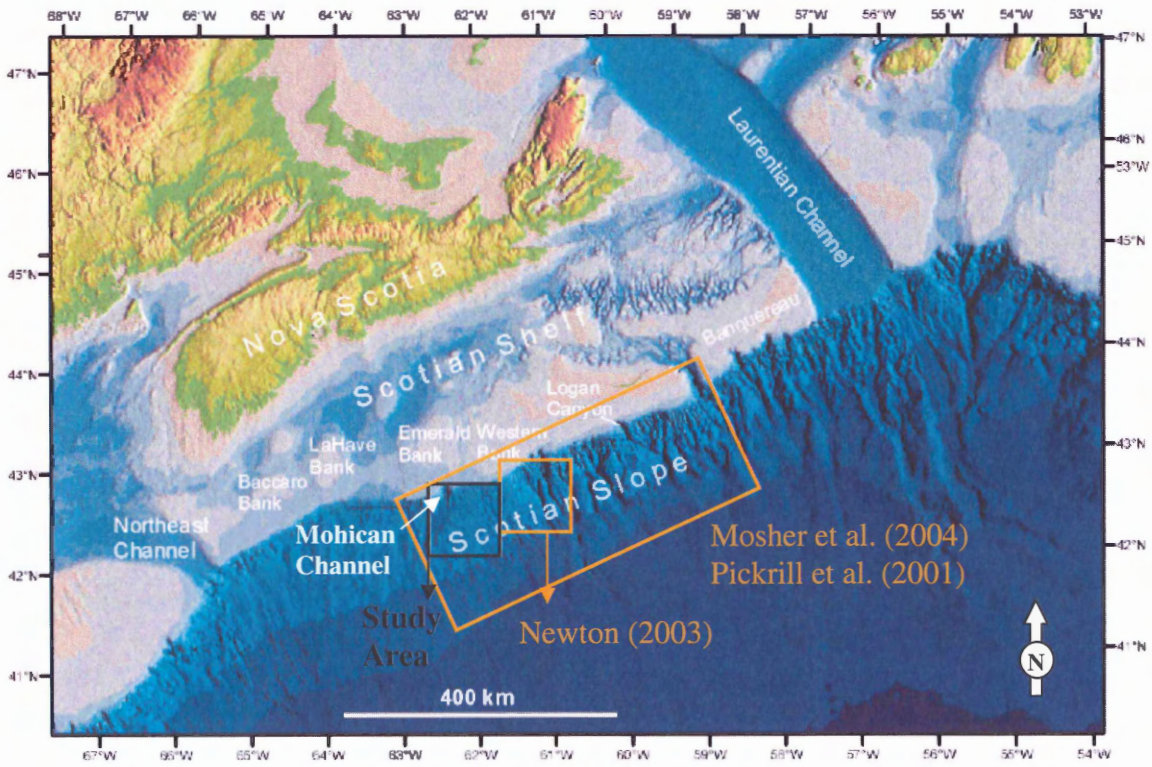

Fig. 1.2 – Regional map of the Scotian Slope with bathymetry. The study area is outlined in black (modified from Campbell et al., 2004). Additional studies referenced within this thesis are labelled in orange. Map projection is Lambert conformal conic.

Piper and Sparkes (1990) first classified the seismic stratigraphy of the Late Cenozoic central Scotian Slope by defining fourteen prominent seismic stratigraphic horizons ranging from early Miocene to late Quaternary. The criterion for the key horizons is to show an abrupt change in seismic facies that could be correlated regionally. A biostratigraphic framework was provided by the Acadia K-62 and Shubenacadie H-100 wells resulting in approximate age control for the seismic stratigraphy. Table 1.1 presents the horizons of Piper and Sparkes (1990) and the approximate ages where biostratigraphic control was applied. Horizons applied to the Mohican Channel study area are highlighted in bold. A synthesis of the biostratigraphic age controls, O^{18} isotope curve, and interpreted seismic stratigraphy of the late Cenozoic are plotted against a geological timescale in Figure 1.3. This figure summarizes known elements of Cenozoic geology on the Scotian Slope to date.

Horizon Name	Approximate Age
Light Red	
Light Yellow	
Brown	
Carmine	Isotopic Stage 6 (First shelf-crossing glaciation)
Flesh	
Rose	
Grey	**Basal Quaternary**
Magenta	
Blue	
Red	**Late Pliocene**
Lavender	Middle Pliocene
Orange	
Pink	Basal Pliocene
Canary	Early Miocene

Table 1.1 – Modified from Piper and Sparkes (1990), the table illustrates all horizons defined within the Cenozoic seismic stratigraphy. Horizons in bold are those applied to the study area

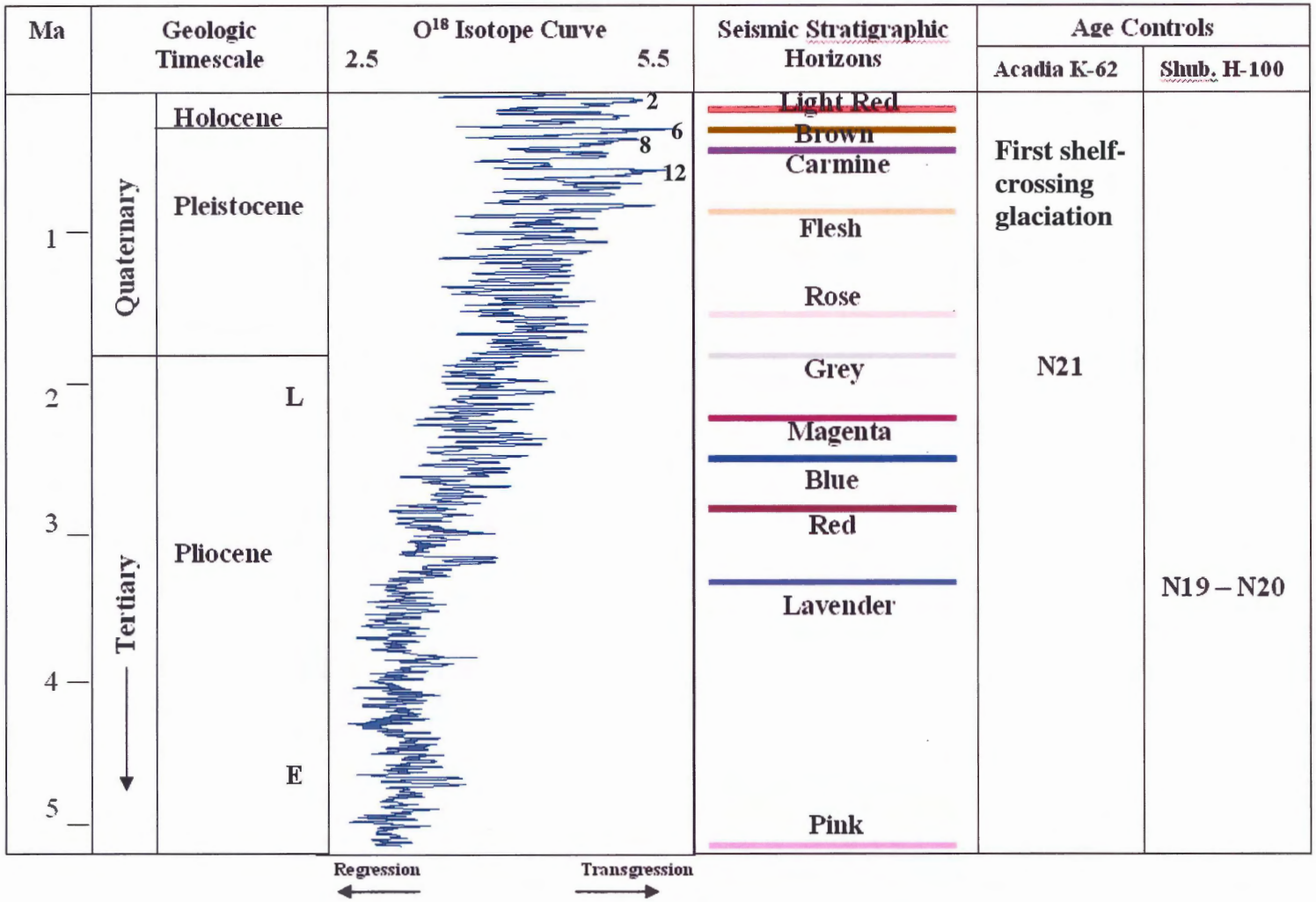

Fig. 1.3 – Synthesis of data to date on the central Scotian Slope shows a reference oxygen isotope curve (Shackleton and Pisias, 1985) from Greenland ice-core, seismic stratigraphic horizons (Piper and Sparkes, 1990), and biostratigraphic age control from planktonic foraminiferal assemblages N19-N21 (Piper and Sparkes, 1987). Abbrevation 'Shub' represents Shubenacadie. Interpreted oxygen isotope stages are indicated numerically on the curve.

Additional studies in this region of the Scotian Slope have been completed by Gauley (2002) and Newton (2003). Newton (2003) described the stratigraphic framework of an area directly east of the Mohican Channel study area based on the key horizons of Piper and Sparkes (1990). The horizons of his work are those used to directly correlate into the study area.

1.4 Geological Setting

1.4.1 Tectonic and Stratigraphic Evolution

The Scotian Slope is part of the passive continental margin, formed during the Mesozoic rifting of the Atlantic Ocean. Deposition within the Scotian basin first began in the mid-Triassic with red beds and evaporates over which lie thick successions of Jurassic and Cretaceous strata (Wade & MacLean, 1990).

Three significant periods of basement subsidence occurred in the Jurassic, Cretaceous and Tertiary respectively, resulting in several sedimentary sub-basins on the Scotian margin. Of these, the most significant sediment depocenters are the Sable, Abenaki, Laurentian and Shelburne sub-basins, which are located several hundred kilometres offshore Nova Scotia (Louden, 2002). Specifically, the Mohican Channel study area lies over the eastern reaches of the Shelburne sub-basin as seen in Figure 1.4 below.

Total sediment thickness varies over the Scotian margin and is illustrated in Figure 1.4. To the west, sediment is thickest along the continental slope and rise and to the east the thickest sediment occurs on the outer shelf. This thickening variation may be

explained by a variable response of the margin to changing patterns of crustal and lithospheric thinning during rifting (Louden, 2002).

The Scotian margin is seismically stable and volcanically inactive. The major dynamic structural factor is salt tectonics of the underlying Argo Formation salt of Triassic age. Figure 1.5 illustrates the summarized stratigraphic synthesis of the Mesozoic and Cenozoic Scotian Slope geology (Kidston et al., 2002).

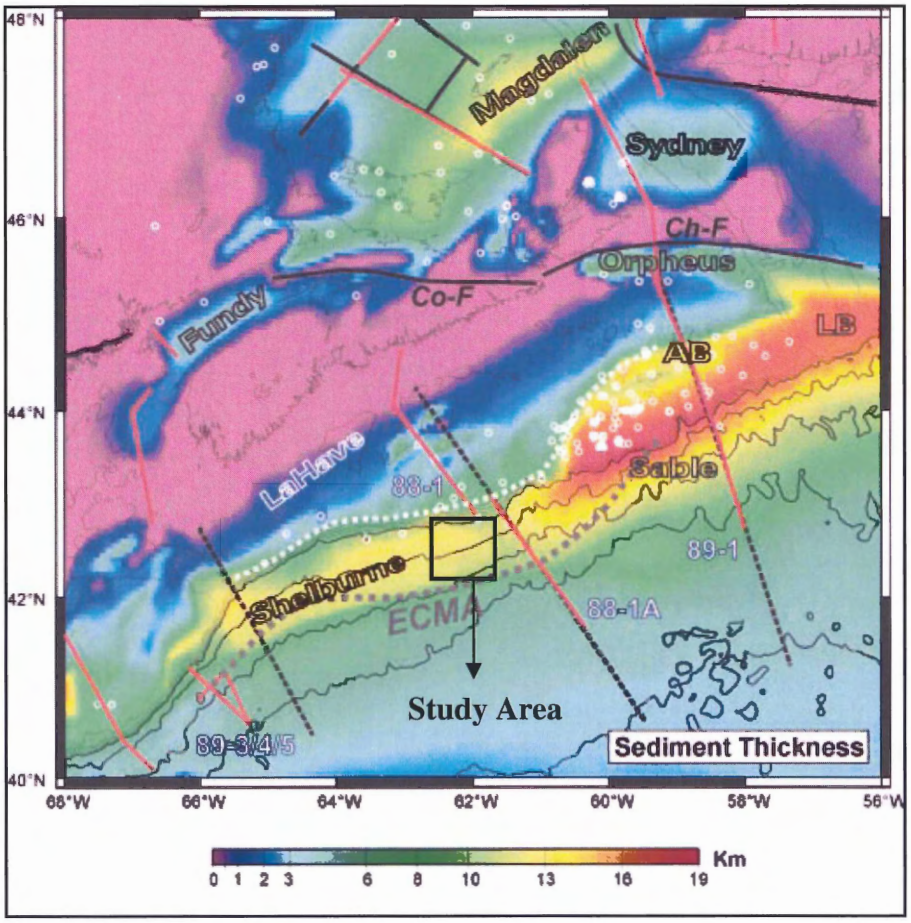

Fig. 1.4 – Total sediment thickness map of the Scotian Margin. Major sub-basins are labelled and the study area is outlined in black. White circles represent offshore wells. Modified from Louden (2002).

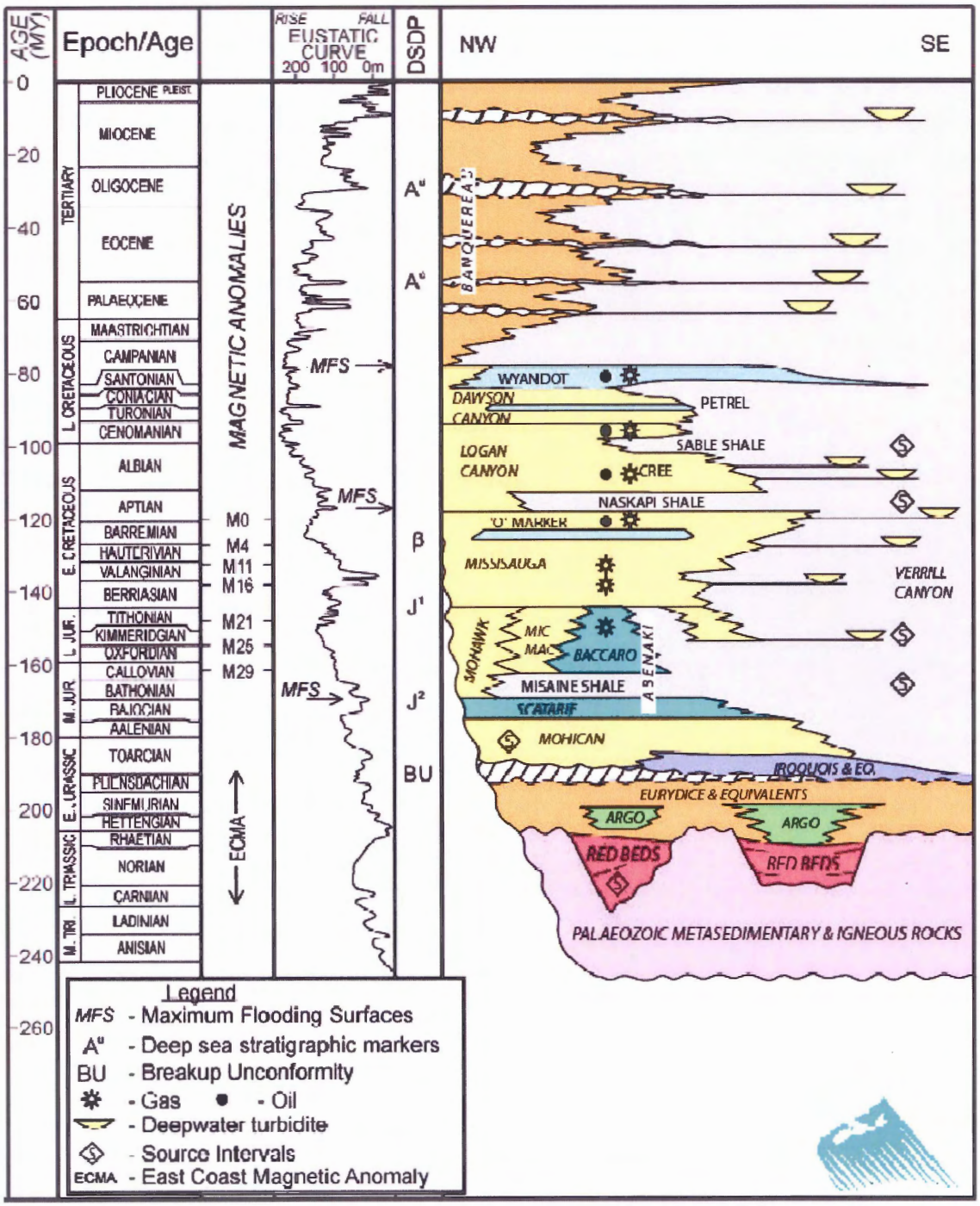

Fig. 1.5 – Synthesis of the stratigraphy and eustatic sea level curve for offshore Nova Scotia, correlated with the geological time scale illustrates the geology of the Scotian Slope throughout the Mesozoic and Cenozoic (Kidston et al., 2002)

1.4.2 Late Cenozoic Geology

Sea level lowstands throughout the Tertiary period resulted in an accumulation of prodeltaic shales and deep canyon incision on the Scotian Slope (Mosher et al., 2004). Rapid deposition on the slope developed at the commencement of terrestrial glaciation in the Pliocene, followed by extensive gully incision that marked the base of the Pleistocene. Throughout this time, the primary depositional environment continued to be that of a prodeltaic system (Mosher et al., 2004). In the mid-Pleistocene, at approximately 0.5 Ma, the first shelf-crossing glaciation took place marking the onset of glacial influence directly on the continental slope (Piper, 2001). Fluctuating ice-margin advances and retreats throughout the mid-late Pleistocene resulted in varying sedimentation processes. Much of the section is dominated by the rapid proglacial sedimentation of glacial advances and retreats, whereas slow accumulation of hemipelagic sediment was typical of interglacial highstands (Mosher et al., 2004). The rapid deposition characteristic of glacial stages corresponds with periods of slope instability; consequently, mass wasting events played an important role in the evolution of the Pleistocene Scotian Slope (Mosher, 1987).

The last glacial stage to affect the Atlantic Canadian margin is known as the Wisconsinan glaciation (King and Fader, 1986). Its final retreat from the continental shelf has been documented at approximately 16 ka (MacDonald, 2003). Deposition of sediments after influence of the glaciations was removed is termed post-glacial sedimentation and is dominated by hemipelagic and pelagic sedimentation that continued from the Late Pleistocene through the Holocene (Mosher et al., 2004). Consequently, sedimentation rates have been significantly slower throughout this postglacial stage and

instances of slope instability have decreased. Few Holocene mass failure deposits have been documented in comparison to those of the Pleistocene (Pickrill et al., 2001).

1.4.3 Surficial Geology and Morphology

Pickrill et al. (2001) and Mosher et al. (2004) studied the surficial geology of the Scotian Slope through a collaborative high-resolution multibeam survey that encompassed the Mohican Channel study area. The survey revealed a smooth topography compared to that of the eastern Scotian Slope. There is a significant absence of canyons; however, several escarpments have been observed that presumably represent slide failure scars (Mosher et al., 2004). The slope gradient in this area is uniquely constant from the shelf break to continental rise. Rotational sediment slumps were observed mid-slope at approximately 600-1000 m below sea level. At this same depth, pockmarks are also abundant. Their presence is thought to be a result of escaping fluids via deep faults or gas escape from a gas hydrate cap. In greater water depths of 2000-2500 m below sea level, large failure scarps are present (Pickrill et al., 2001). Specifically, in the southwest of the study area there is an example of a linear scarp located along a shallow fault zone. The escarpment ranges up to 80 m in height, and spans a lateral distance of several ten's of kilometres (Mosher et al., 2004). This feature is associated with a mass failure deposit of Late Pleistocene age and is noted, along with other morphological characteristics, within Figure 1.6.

Interpretations of piston core samples show a drape of Holocene and Late Pleistocene fine-grained sediment throughout the study area. These sediments overlie

several different facies such as proglacial muds with ice-rafted sediments, rotational slump blocks, debris flows, or older eroded surfaces (Pickrill et al., 2001).

Both Pickrill et al. (2001) and Mosher et al. (2004) have concluded that significant sediment failure is uncommon within the Holocene, but is common throughout the Pleistocene. Their studies have shown that the largest failure scarps are likely tens of thousands of years old, although some have been documented at younger ages of 12-15 ka. Younger sediments overlying the scarps have accumulated to tens of metres indicating a significant time of stable deposition (Pickrill et al., 2001).

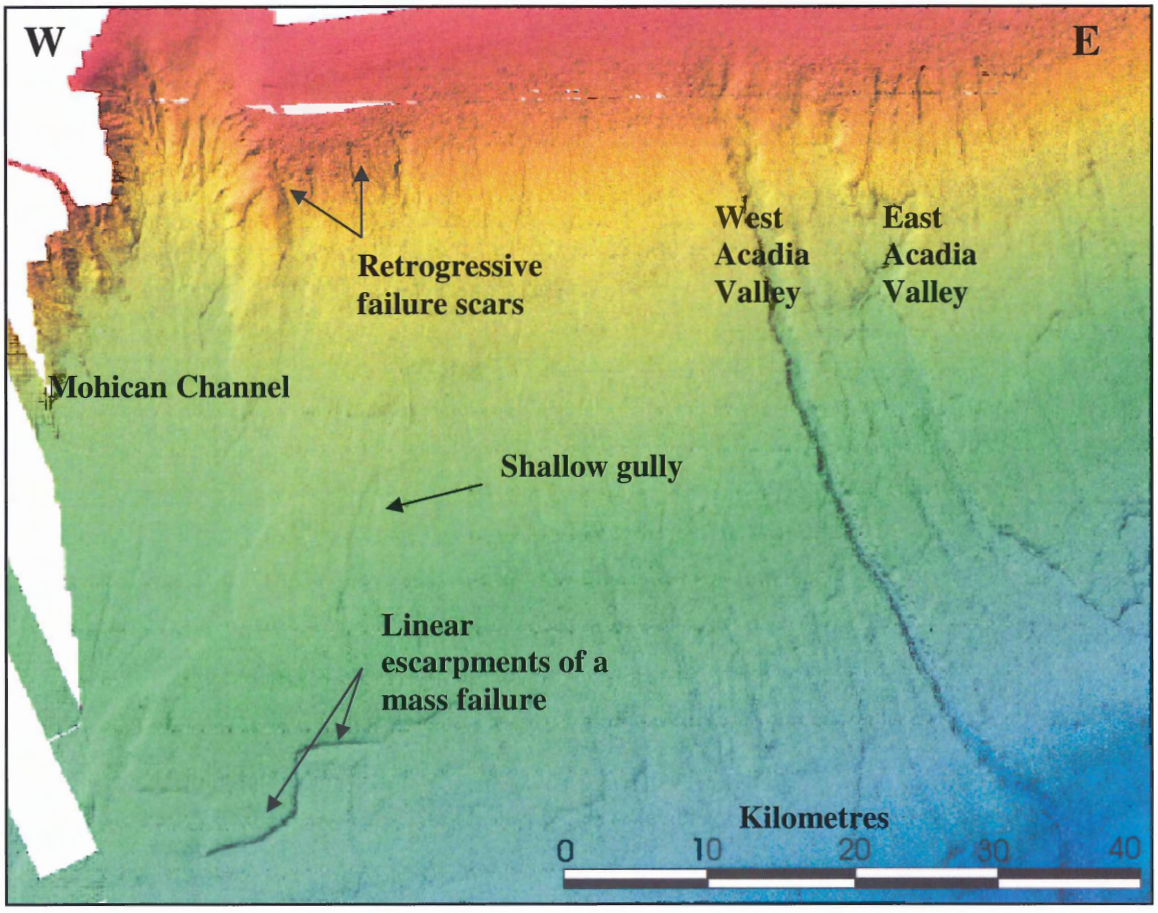

Fig. 1.6 – Multibeam render of the study area, with significant morphological features highlighted. Modified from Campbell et al. (2004)

CHAPTER 2

METHODS

2.1 Introduction

The two major seismic techniques employed in this study are: 1) conventional two-dimensional seismic surveying and 2) seismic surveying with the digital deep-towed hydrophone (DDH). Both are used by the Geological Survey of Canada (Atlantic) in marine surveying, however, the DDH is in an experimental stage of development and its use is currently limited. The applicability of this method to defining seismic stratigraphy is an objective of this study.

2.2 High-resolution Seismic Surveying

Two-dimensional (2D), high-resolution seismic reflection sections are the primary data source for developing the stratigraphy within this study and interpreting the sedimentological processes involved. The various elements involved in this seismic stratigraphic analysis include data acquisition, processing and interpretation. The seismic surveys acquired within the study area are outlined in Figure 2.1.

2.2.1 Seismic Reflection Acquisition

A two-dimensional marine seismic reflection system consists of three major components: (1) a sound source, (2) a hydrophone receiver, and (3) a recording apparatus. The source and receiver are towed in the water behind the survey vessel (Fig. 2.2). The basic principle behind the system follows that an acoustic signal is emitted from the seismic source; upon reaching the seafloor, part of the acoustic energy is

reflected while some of it penetrates into the underlying material. The amount of energy reflected is dependent upon the density and velocity contrast, or acoustic impedance contrast, of the seafloor-water column interface. The portion of the signal that penetrates into the sediments then follows a similar pattern, some reflecting off interfaces of high impedance contrast and some transmitting further into the sediment until the signal is completely attenuated. Reflected signals are recorded in the hydrophone receivers and are digitized either at the receiver or transmitted to a shipboard digitizer on the survey vessel to be gathered into a seismic section.

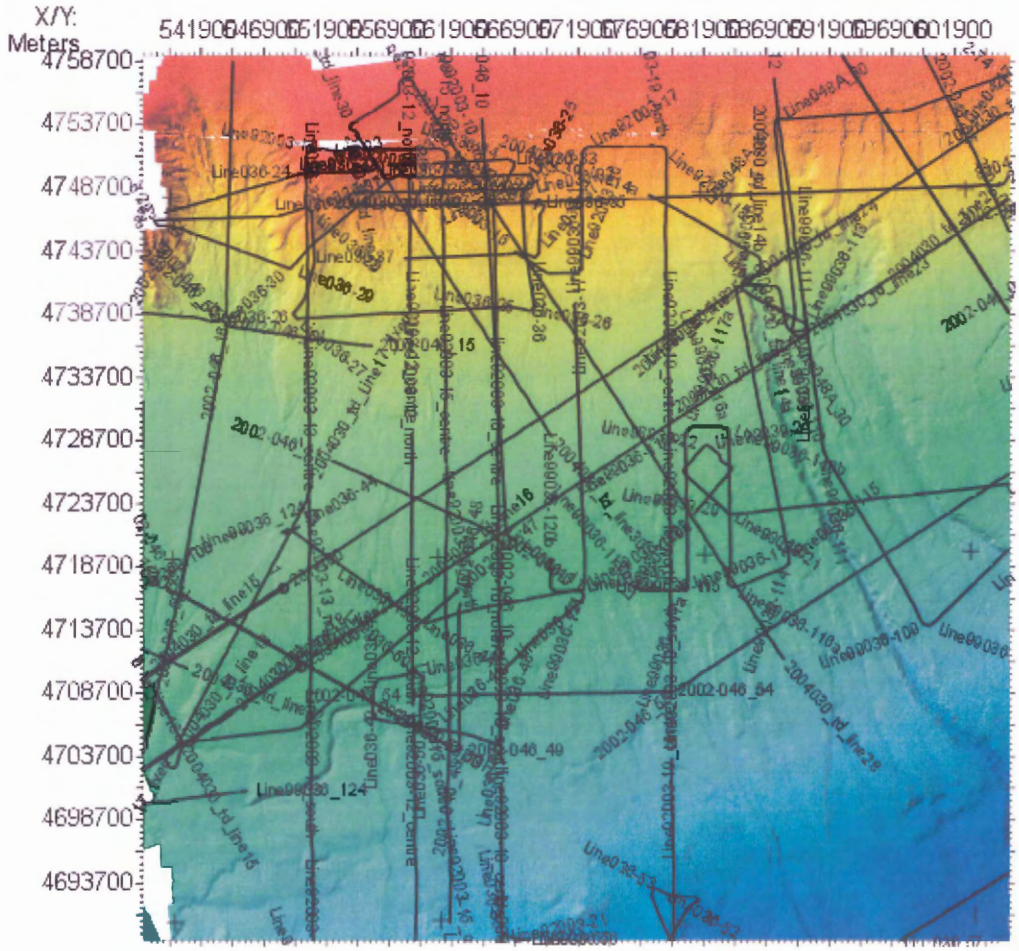

Figure 2.1 – 2D seismic reflection lines acquired within the study area are shown in black. All lines were acquired by the Geological Survey of Canada (Atlantic) on board the CCGS Hudson. Colours refer to multibeam bathymetry: red represents shallower water depths of the continental shelf and blue represents greater water depths of the lower slope

All reflection seismic lines used within this project have been acquired by the Geological Survey of Canada (Atlantic) on board the research vessel CCGS Hudson. The latest survey, CCGS Hudson Cruise 2004_030 has provided the most valuable regional seismic lines for this study; therefore, details of the methods used during this expedition will be presented. Additional data are provided from CCGS Hudson Cruise 2000_042, Cruise 2001_048 and Cruise 2002_046, in which acquisition techniques were very similar.

2.2.2 Seismic Source

Most data used in this investigation were acquired with pneumatic sources such as sleeve guns or Generator Injector (GI) guns, which are both shown in Figure 2.3.

The sleeve gun, a type of airgun acoustic source, operates by a sudden release of pressurized air from an enclosed chamber, which generates a pressure wave in the surrounding water. The sleeve gun array generally consists of two 40 in^3 airguns towed roughly 20 m behind the vessel. This array is mounted 0.45 m under a tow sled with 0.75 m spacing between guns. At rest, the guns sit at a depth of 3.75 m below sea level, however in motion they may surf at shallower tow-depths (Mosher, 2000).

The GI gun generates an initial blast of pressurized air similar to a conventional airgun followed by a secondary air blast to improve the source signature. The initial compressed blast of air forms the primary pulse and begins to expand. When the bubble reaches its maximum volume, it envelops the injector ports of the gun and results in an internal pressure much less than the surrounding hydrostatic pressure. The bubble from a conventional airgun would collapse from this pressure difference resulting in a rhythmic

pulse of expansion and collapse. This oscillation is known as the bubble pulse effect and is seen in the resulting seismic data as an interfering artifact. The GI gun, however, will fire its injector at the moment the bubble reaches its maximum size, forcing more air inside. This increase in internal pressure prevents a major collapse of the bubble thereby reducing the oscillations of the air blast (Mosher, 2005). Generally, two GI guns are used in an array and are mounted on an I-beam approximately 2 m apart and 0.5 m beneath the sled. Two Norwegian floats are attached to the beam for buoyancy in the water and result in a tow-depth of approximately 2.5 m below the sea level (Mosher, 2005).

2.2.3 Receivers

A Teledyne streamer, a segment of which is illustrated in Figure 2.3, contains the hydrophone receivers used in seismic acquisition. The streamer is 61 m in length, with an 8 m dead section at the head and a 5 metre dead section at the tail. The resulting 48 m of active streamer consists of 3 sets of 2 interlacing hydrophone groups. Each group contains 16 individual hydrophones that are separated by 1 m. The signals received from the active groups are summed into a single channel and transmitted onboard the ship (Mosher, 2005).

Attached to the Teledyne streamer at the lead-in section is a DigiCourse DigiBird Model 9000-5010. This piece of equipment enables manipulation of the streamer's tow depth. For most operations the bird is set to maintain a tow-depth of approximately 4 m to be compatible with the depth of the airgun (Mosher, 2005). Figure 2.2 illustrates the geometry of the source and receivers in a standard 2D seismic reflection survey.

2.2.4 Digital Recording

Prior to digitizing, the signal transmitted from the hydrophones is not filtered or amplified. The GSCDIGS unit (Figure 2.3) digitally records the seismic signal, providing high sample rates and dynamic range (Mosher, 2005). Navigation data and delay times are immediately read into the system and, after recording, the data are ready for processing and interpretation. In the past, data were recorded to tape; however, recent data is recorded to DVD media.

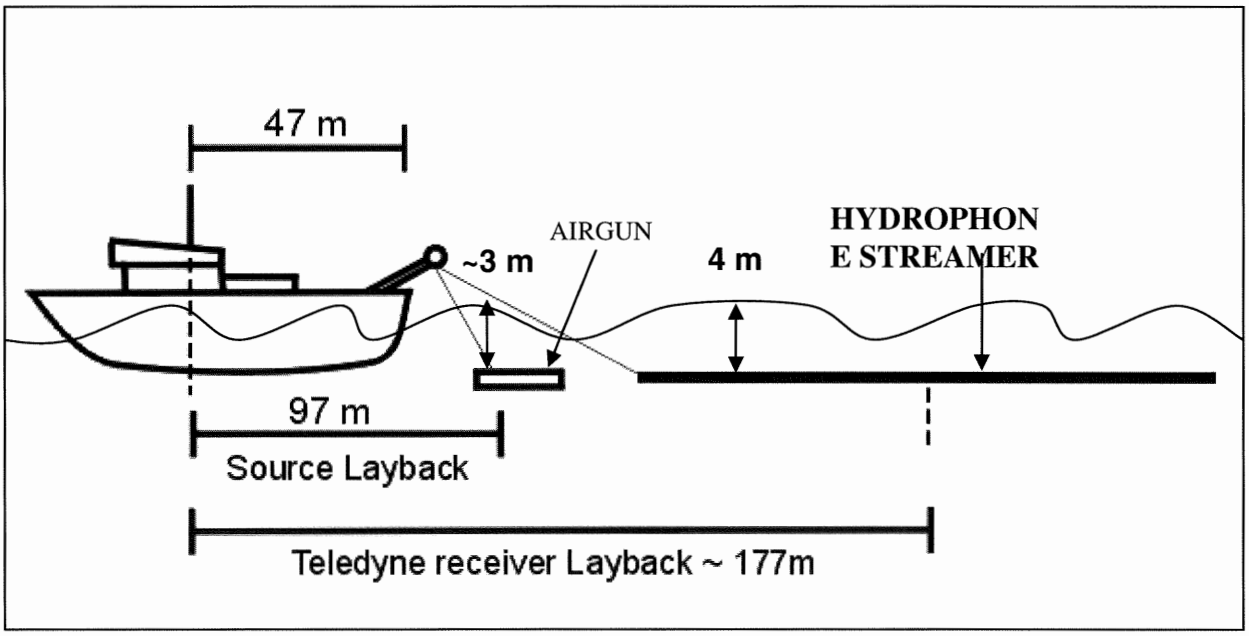

Fig. 2.2 – Schematic diagram of the reflection seismic survey geometry. (Modified from Mosher, 2005)

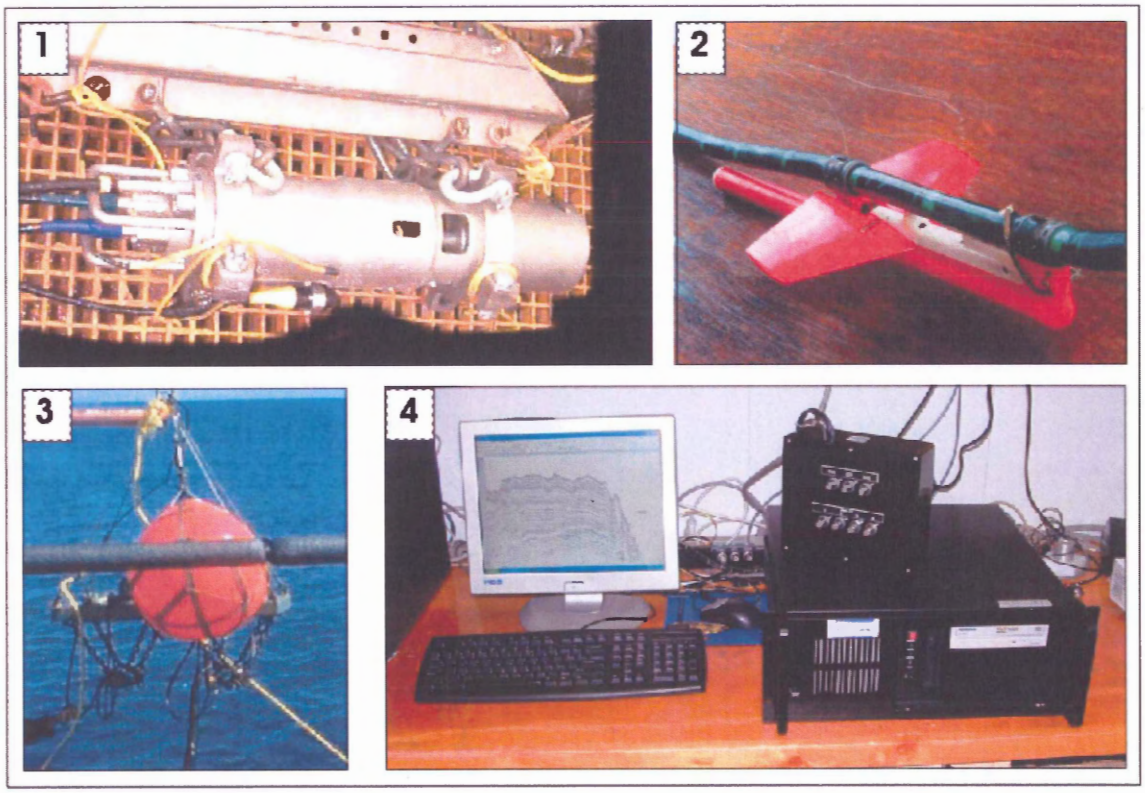

Fig. 2.3 – Components of the seismic acquisition system include **1)** airgun (GI gun), **2)** receivers (Teledyne streamer with attached Digicourse bird), **3)** airgun (sleevegun array with a Norwegian buoy), and **4)** onboard digitizing system (GSC DIGS).

2.2.5 Seismic Data Processing

Seismic data from the tape or DVD media are extracted and imported into Seismic Micro-Technologies™ Kingdom Suite 2D/3D Pak interpretation software. Processing the high-resolution data into readable sections primarily consists of bandpass filtering to eliminate undesirable noise. This basic processing is performed within the Kingdom Suite software. After analyzing the frequency spectrum of a particular seismic section, a band-pass filter is applied. Generally, the dominant frequency ranges between 35Hz and 250 Hz therefore a bandpass filter with a low-

end cut of 35 Hz and high-end cut of 350 Hz is suitable and results in a legible seismic section, ready for interpretation.

2.2.6 Seismic Interpretation

Seismic Micro-Technologies™ Kingdom Suite interpretation software is also used for defining seismic stratigraphy in the study area. Seismic stratigraphic horizons, denoted by coherent high-amplitude reflections and abrupt changes in acoustic character, are defined with specific colour markers. Six key horizons are extended from the study area of Newton (2003) and were correlated into the Mohican Channel study area.

There are different modes offered in Kingdom Suite for picking horizons. The mode most useful for the purposes of this study is an auto-pick fill mode. This mode allows for manual definition of certain points on a reflection event, between which the computer interpolates a horizon locking to specified attributes of each seismic trace. Depending upon the acoustic character of a specific horizon, both absolute peaks and troughs of the wavelet were traced. Faults can also be highlighted by Kingdom Suite, but this feature was used minimally within the scope of this study.

The generation of isochron maps is a useful feature of Kingdom Suite. Each key horizon in the study presumably represents a synchronous surface, therefore the data between these horizons represents a unit of material that has been deposited over a uniform time interval and is referred to as an isochron. By mapping a regional grid of each key horizon, a map indicating the thickness of the seismic stratigraphic intervals in two-way travel time between the horizons can be generated. Although these grids do not represent unit thickness in depth measurements (metres), the two-way travel time

(seconds) is assumed to be proportional and is indicative of depositional style and accumulation pattern of sediment.

2.3 Digital Deep-towed Hydrophone

The digital deep-towed hydrophone (DDH), an experimental seismic acquisition system tested within the study area, presents several challenges throughout data acquisition and processing. The methods to develop interpretable DDH sections vary significantly from those of conventional reflection seismics described in the previous section.

2.3.1 DDH Acquisition

The DDH system uses the same pneumatic source as conventional seismic systems; operating either sleeve guns or Generator Injector airguns. The source is towed at the same level, approximately 4 m below the sea level and 20 m off the stern of the vessel.

In DDH acquisition, the positioning of the hydrophone receiver is considerably different from conventional seismic surveying. The goal of the DDH is to tow the hydrophones as close to the seafloor as possible. Aboard the CCGS Hudson, approximately 2000 m of cable are accessible on the winch. This amount of cable enables the hydrophone to be towed at an approximate depth of 1000 m, travelling at a speed of 2.5 knots. The receiver system used was comparably shorter than that of conventional seismic acquisition and measured 3.7 m (12 ft) with hydrophone spacing of 0.2 m (6 in.), with a total of 24 hydrophone receivers.

The signal received by the hydrophones at depth is digitized prior to transmission onboard the surveying vessel. Traditionally, surface seismic systems broadcast the raw analogue signal immediately for onboard digitizing. Digitizing at depth is beneficial as it minimizes the loss of signal through the cable in the water column and eliminates electrical interference and other sources of noise during transmission. The digitizer is enclosed in a pressure case at the lead of the hydrophone streamer and secured to a core head weighing roughly 1000 kg. Telemetry transmitters and receivers placed at the ends of the cable exchange the digitized seismic signal with little error (Mosher, 2000). Figure 2.4 illustrates the different survey geometries of conventional and DDH systems.

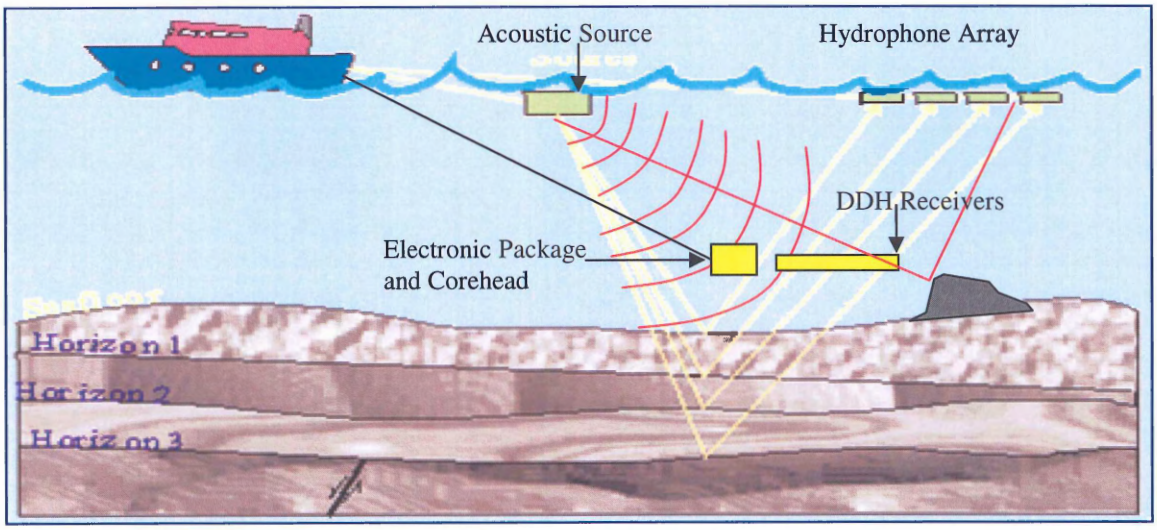

Figure 2.4 – Diagram demonstrating the difference in geometry between DDH and conventional surface seismic systems (Mosher, 2005).

2.3.2 DDH Data Processing

The DDH system is new technology with the promise of enhanced resolution of seismic data, but with any new technology there are some challenges. Data processing encompasses several of these challenges.

In order to compensate for changing bathymetry, the tow-depth of the receiver is altered to keep the streamer as close to the seafloor as possible, without collision. These depth variations result in a seismic section without depth compensation, with multiple delay changes, and with improper reference to the seafloor. Figure 2.5 illustrates the irregular nature of the raw DDH data. Secondly, properly referencing the DDH survey is difficult owing to the lack of navigation data to denote the streamer position. The layback of the receiver behind the vessel is unknown for several reasons; the length of cable leading to the streamer is not measured, it is not constant, and it is not linear with layback. However, the time of the seismic shot, ship's position and tow depth of the streamer are known. These established variables aid in referencing the sections to proper navigation data.

2.3.3 Filtering

DDH processing is conducted with SISimage Vista seismic processing software. The first step to processing the data is common to most seismic data. Filtering is the removal of undesirable signal, or noise, within the section. Signals from external sources such as ship noise and ocean wave action can obscure the geological signal. To eliminate these effects, a bandpass filter of 60-1000 Hz is applied to the seismic data. This filter removes all signals below 60 and above 1000 Hz, which are characteristic of these external influences. The result is a cleaner render of the seismic section.

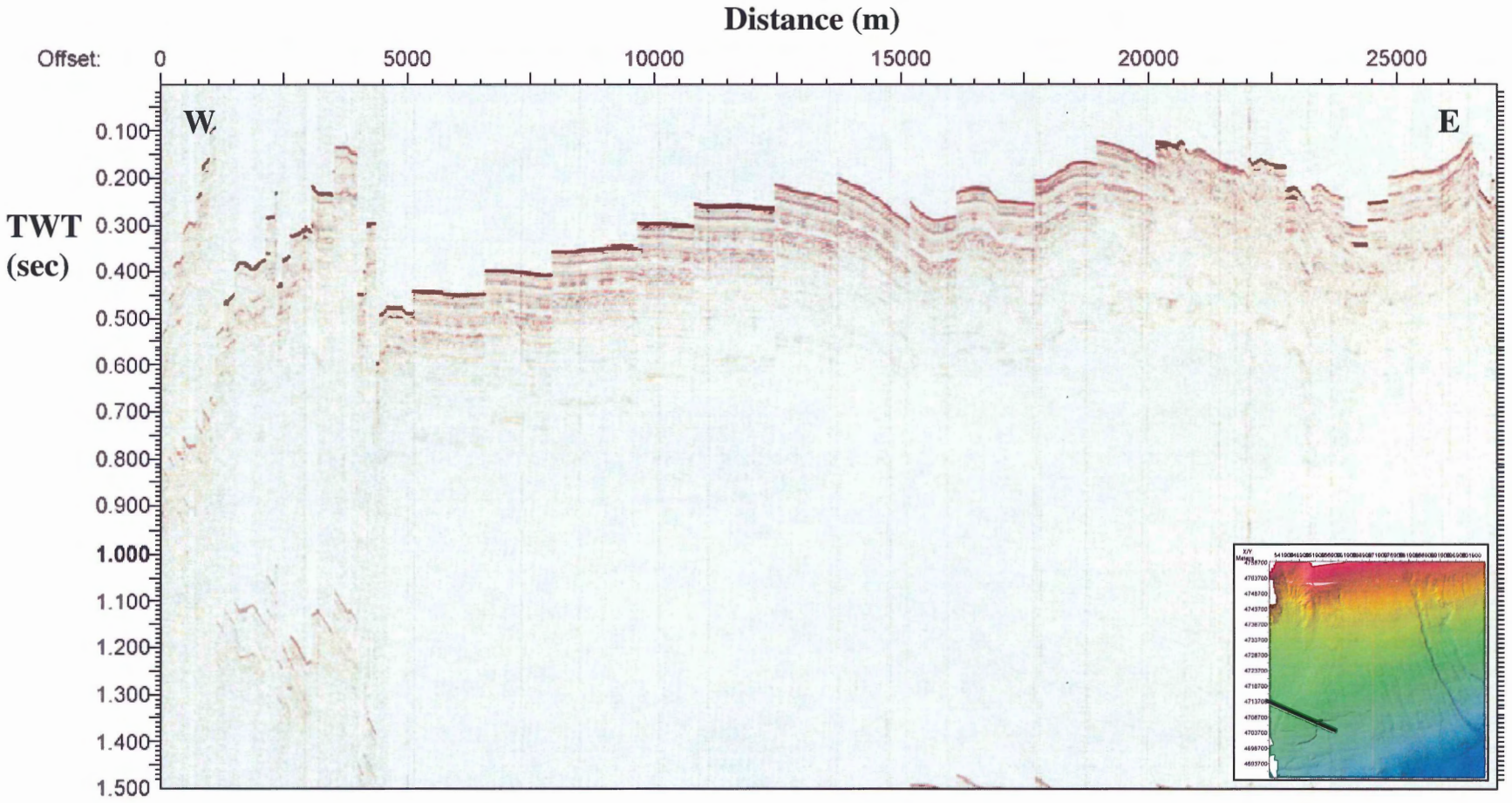

Fig. 2.5 – Unprocessed DDH data, CCGS Hudson Cruise 2002_046 Line 53. Inset map indicates the location of the line in the study area.

2.3.4 Referencing to Navigation Data

After filtering, the DDH line is properly referenced to navigation data. This is an involved method because the streamer position is unknown. To overcome this, the DDH data are compared to equivalent surface seismic data. Drawing comparisons on the raw data is not possible therefore both the surface and DDH sections are flattened to a horizontal seafloor. At this time, it is possible to correlate specific geological features of the DDH section to those of its equivalent surface seismic section. Based on the positioning of these distinct seismic features, a proper navigation file is generated from the ship's track to represent the position of the DDH data.

2.3.5 Static Correction

Once positioning of the data is determined, the third step to processing a DDH line is fitting the profile to the seafloor morphology. To make the proper depth corrections for the seismic section, regional bathymetric data are required. Data from the corresponding surface seismic profile can also be used. Within the Mohican Channel study area there are sufficient bathymetry data. A static correction, within the Vista software, is applied to the seismic traces in the DDH profile based on the depth to seafloor at the position of each trace. This process has been successful in reconstructing the seafloor and integrity of the DDH seismic section.

2.3.6 Deconvolution

An advantage to the unconventional geometry of the DDH system is that the receiver records the direct arrival of the source wavelet prior to its reflection from the

seafloor. This wavelet is the best representation of the source signature and each trace of the seismic section is deconvolved with its corresponding source wavelet. The purpose of deconvolution is to minimize the effect of the source signature on the seismic reflection record. This produces a clearer, high resolution seismic section.

In an effort to optimize the quality of the DDH section, several deconvolution trials were attempted by varying a few parameters in the mathematical operation. The source wavelet was successfully collapsed and the reflections within the seismic data were subsequently sharpened. For clarity, Figure 2.6 illustrates the complete DDH processing workflow applied in this study.

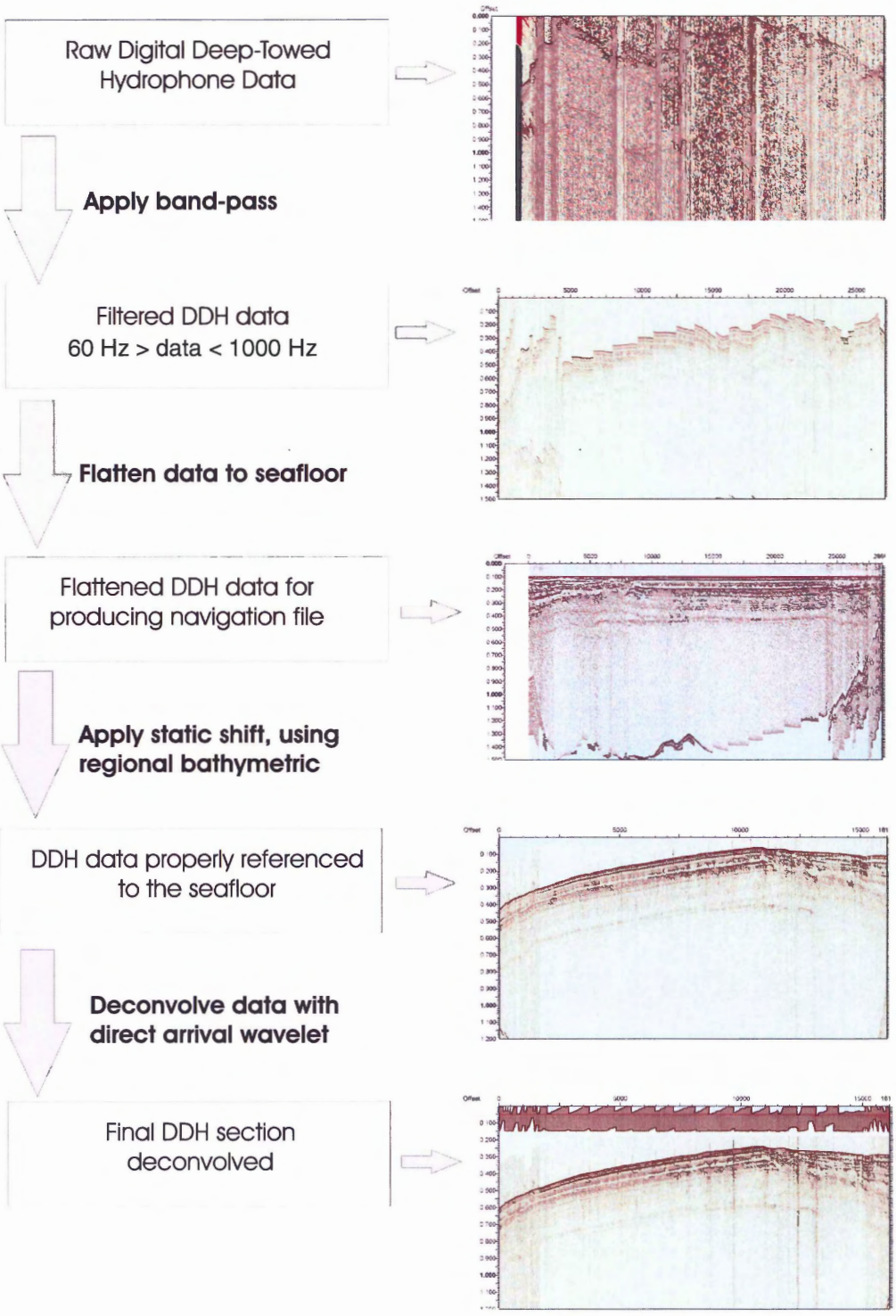

Fig 2.6 – Work flow showing the DDH processing method. The data shown is from Line_53 of Hudson Cruise 2002_046.

CHAPTER 3

RESULTS

3.1 Introduction

The approach taken within this study to interpret 2D seismic data is that of an industry standard. The following workflow (Figure 3.1) outlines the steps involved in seismic interpretation that are presented in the study. This chapter specifically discusses seismic stratigraphy, seismic facies and structural elements such as faults. The seismic data provided by the DDH acquisition technique are presented and subsequently compared to those of conventional 2D reflection seismic data.

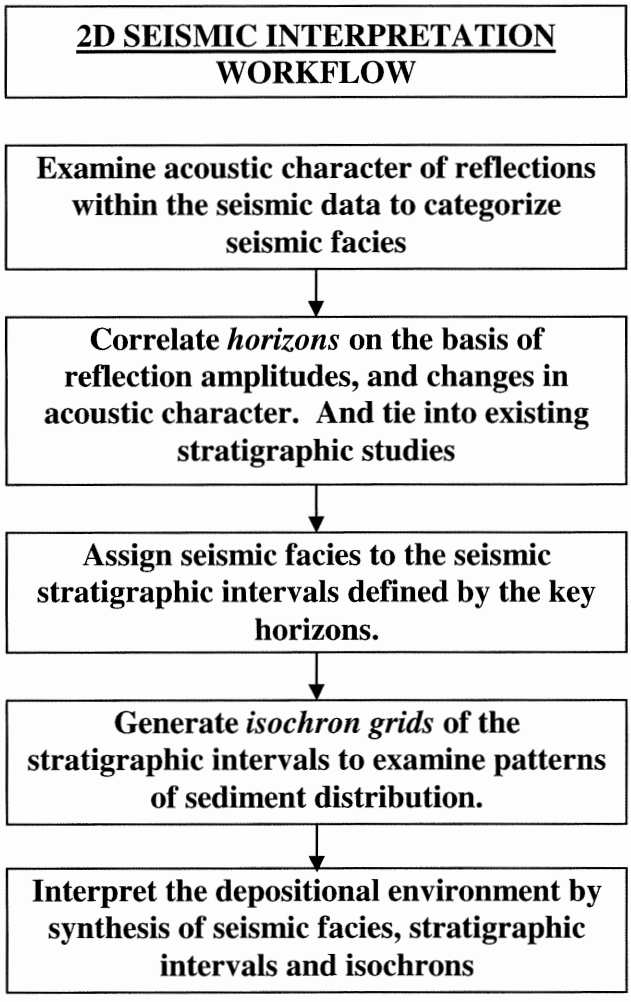

Fig. 3.1 – Representation of the 2D seismic interpretation workflow.

3.2 Seismic Facies

A seismic facies is defined by three major attributes: 1) reflection configuration, 2) reflection continuity, and 3) reflection amplitude (Reading, 1986). Six different seismic facies have been observed from the seismic stratigraphy within the study area and have been designated Facies A through F. They are illustrated in Figure 3.1.

Facies A contains continuous parallel reflections of significantly high amplitude. Facies B is composed of similarly continuous parallel reflections; however they are of comparably lower amplitude. Typically, Facies A directly overlies Facies B in seismic section resulting in cyclical sequences. Facies C is composed of chaotic, discontinuous, high amplitude reflections, with little to no internal structure. Facies D contains similar chaotic reflections; however they are of significantly lower amplitude. This seismic facies is generally capped by discontinuous high amplitude reflections of variable relief. Facies E consists of sub-parallel, discontinuous, low amplitude reflections that are overlain by high amplitude reflections. The overlying reflections have discontinuous, hummocky relief in strike section; however they are generally continuous and flat, down-dip. Facies E is the only seismic facies in this study to demonstrate differing acoustic character along strike versus down dip. Finally, Facies F consists of high amplitude reflections and is typically only observed beneath the sediment water interface. The reflections are discontinuous and sub-parallel; roughly equivalent to Facies A with interfingered chaotic intervals.

Facies A – continuous, parallel reflections with high amplitude.

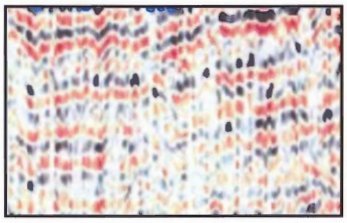

Facies B – continuous, parallel reflections of low amplitude.

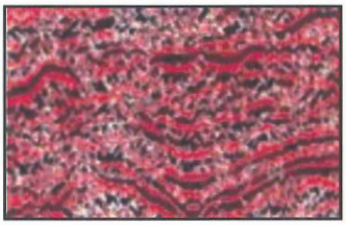

Facies C – high amplitude, chaotic reflections.

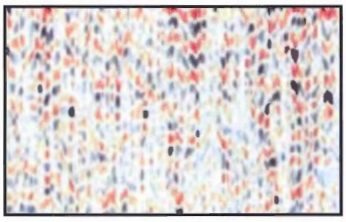

Facies D – low amplitude, acoustically transparent chaotic reflections, lacking internal structure.

Facies E – somewhat chaotic reflections capped by high amplitude, hummocky reflections.

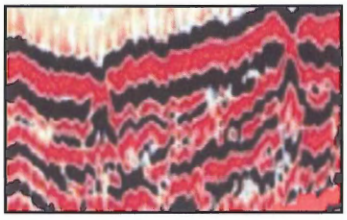

Facies F – sub-parallel, discontinuous, high amplitude reflections with chaotic intervals.

Figure 3.2 – The six seismic facies within the study area and the description of their acoustic character

3.3 Key Horizons

Piper and Sparkes (1990) previously correlated key horizons on the Scotian Slope that are used to define seismic stratigraphy in this study. In the vicinity of the Acadia Valley system, nine horizons have been identified; from oldest to youngest, the horizons are named red, blue, magenta, grey, rose, flesh, carmine, brown and light red. Of these horizons, six were directly tied into the Mohican Channel study area. Three horizons, including rose, flesh and carmine of Newton (2003) are not present in this study area as a result of erosion by the Acadia Valley system that separates the two study areas, and truncation by a regional mass transport flow. The flesh and carmine horizons are absent west of the West Acadia Valley, while the rose horizon is absent both to the south and west of the head of the mass transport deposit that lies between the grey and brown horizons. Variable sedimentation patterns impeded correlation; however, six horizons have been successfully traced to the western edge of the study area bounded by the Mohican Channel. These horizons define six seismic stratigraphic units, which will be described in more detail below.

Biostratigraphy from the Acadia K-62 and Shubenacadie H-100 wells supplies age control for some key horizons (Piper et al., 1987). Planktonic foraminiferal assemblages denote the red horizon as mid-Late Pliocene in age, and the grey horizon as the base of the Pleistocene (Piper et al., 1987). The carmine horizon, which has not been correlated regionally within the study area, is denoted as 0.45 Ma; approximately mid-Pleistocene in age.

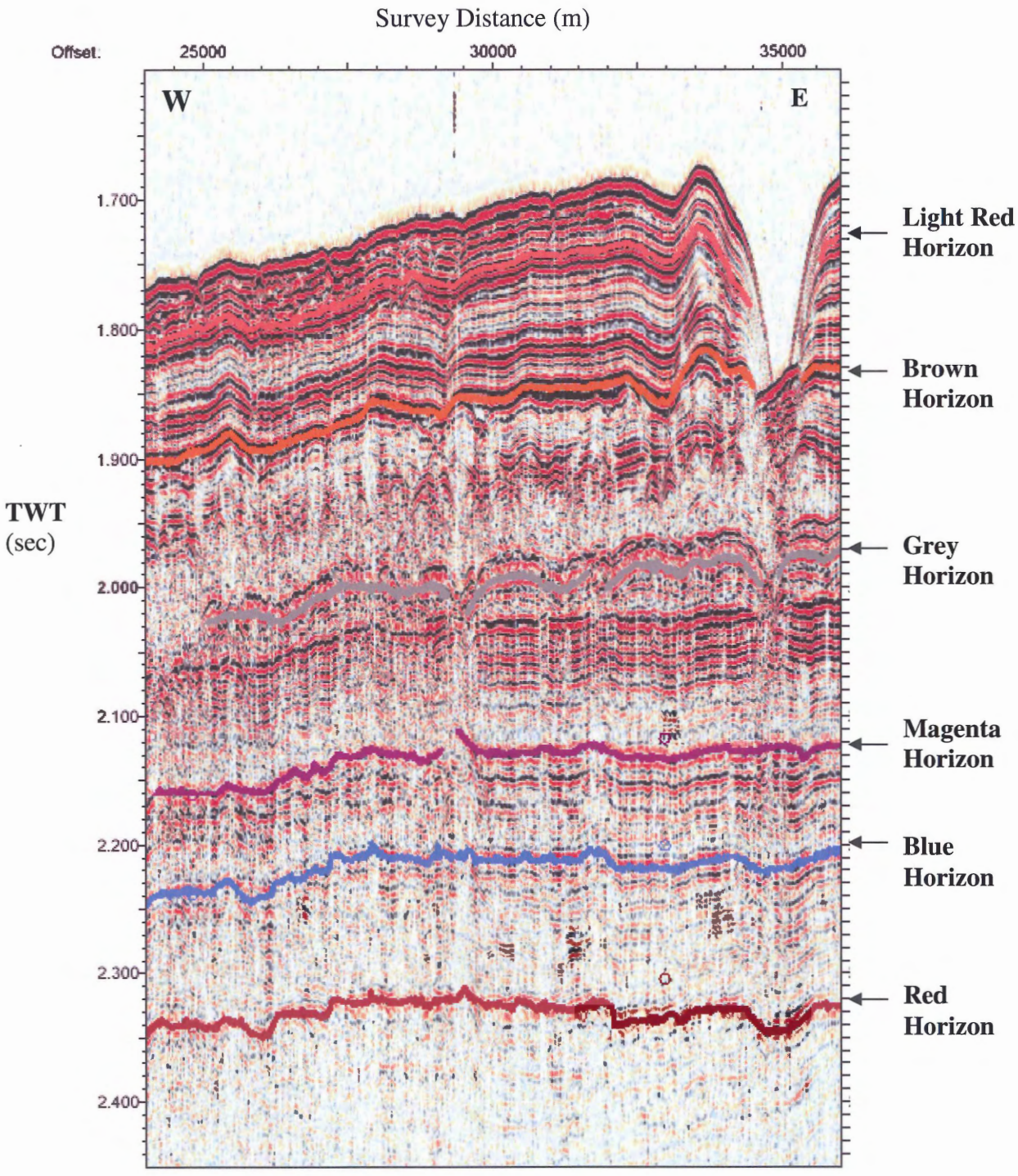

Figure 3.3 – Example of a section with all key horizons, taken from survey line 2004030_line23.

3.4 Seismic Stratigraphic Intervals

Six seismic stratigraphic intervals are defined by the correlation of the six key horizons. Interpretation of these intervals requires analyses of the seismic facies, the variability of the interval thickness, and distribution patterns observed in seismic section. Figures 3.4 and 3.5 depict a regional strike and down-dip section respectively, which illustrate the observations made within this section. From oldest to youngest, these intervals are:

Red – Blue Interval

The red-blue stratigraphic unit is difficult to resolve as a result of its depth in the section. Nonetheless, two seismic facies are observed in the interval. Throughout much of the study area, Facies A overlies Facies B in the interval. In down-dip sections, Facies A is significantly thinner than Facies B, and in some sections it is completely lacking. In strike section, the overlying relationship of Facies A on B is continuous from east to west.

Thickness of this interval is slightly variable downslope and does not exhibit notable thinning. On the upper slope it averages 50 ms in thickness, expands to roughly 70 ms on the mid-slope and eventually thins again to its original 50 ms at the base of the slope. Along strike at mid-slope levels, the interval maintains a thickness of about 70 ms from east to west. In the far west of the study area, this interval is eventually truncated by mass failure in the southwest (Fig. 1.6)

Blue – Magenta Interval

Similar to the red-blue interval, this interval contains both Facies A and B but the imaging of the reflections is much improved. Down-dip, most of the upper slope interval

consists primarily of Facies A; however, at mid-slope levels, Facies B emerges at the base of the interval. This relationship remains constant through to the lower slope regions. In strike section, Facies A overlies Facies B to the east but is gradually truncated by overlying reflections.

Thickness of the blue-magenta interval is somewhat constant down-dip with minor thickening in the downslope direction. In strike section, thickness is significantly more variable; average thickness is 80-100 ms to the east and 50 ms to the west. The interval is truncated in the southwest by a mass failure deposit seen in bathymetric data.

Magenta – Grey Interval

The magenta-grey interval contains several seismic facies in variable order. In strike section, Facies E, A and B are present, stacked in order of deepest to shallowest. This stacked relationship is most clearly defined in the eastern portion of the study area. At mid-slope, towards the center of the study area, Facies E and A disappear and the interval thins significantly. Further west along the strike section; however, the stacked sucession of three facies reappear but Facies E is less distinct. Down-dip sections do not reveal the hummocky nature of Facies E. This fact results in the appearance of only two facies down-dip; Facies A overlies B.

The magenta-grey interval thins downslope from a maximum of 130 ms upslope to less than 80 ms at the base of the slope. Laterally, the interval also thins to the west until it is truncated by the southwest mass failure.

Grey – Brown Interval

The grey-brown stratigraphic interval contains the most variable distribution of seismic facies in the study area. The far eastern portion of this interval consists of three

facies. Facies D comprises the base of the unit, above which lies continuous, parallel reflections of Facies A. The top portion of the interval consists of Facies B, the low amplitude equivalent of the underlying Facies A. The entire sequence is capped by the regionally correlatable brown horizon. Towards the centre of the study area, the basal Facies D truncates the grey horizon, suggesting erosion of the underlying interval. Westward of this truncation, Facies A and B are missing and Facies D comprises the entire interval. Generally, the downslope facies variations are equivalent to those from east to west described above. Facies D is the only seismic facies in the interval at the base of the slope.

The thickness of the grey-brown interval generally decreases both downslope and westward. Upper slope thickness averages 200 ms, while it pinches out to less than 30 ms at the base of the slope. To the east, average thickness approaches 200 ms and thins westward to approximately 5 ms before it is truncated by the Mohican Channel.

Brown – Light Red Interval

The brown-light red interval primarily consists of alternating layers of Facies A and B. Generally, Facies A comprises the lowermost layer in the interval, Facies B comprises the mid-interval, and Facies A again comprises the top of the interval. This facies succession is equivalent in both strike and downslope sections.

Thickness of the brown-light red interval tapers from a maximum of 250 ms to a minimum of 50 ms downslope. At mid-slope levels, its thickness varies from 100 ms in the east to 50 ms in the west where the unit is truncated by the mass failure deposit in the southwest of the study area (Figure 1.6).

Light Red – Seafloor Interval

The uppermost stratigraphic interval spans the light red horizon to the seafloor and consists primarily of Facies F. In the far east of the study area, however, the interval gradually changes from the acoustic character of Facies F to that of Facies A. Facies F remains dominant in the western portion of the study area.

The light red - seafloor interval exhibits downslope and westward thinning. The maximum upslope thickness averages 100 ms, while it pinches out completely at the base of the slope. At mid-upper slope levels, the interval thickness varies from approximately 90 ms in the east to roughly 40 ms in the west until it is truncated by the mass failure in the southwest.

Absent Seismic Horizons

The rose horizon, which lies directly above the grey horizon, is truncated by seismic Facies D within the grey-brown interval. It is not possible to correlate the rose horizon because of the lateral extent of the truncating interval. Due to incision by the Mohican Channel and truncation of the horizons at the slope base, they are completely lost in the west of the study area.

During correlation of seismic horizons from the study area of Newton (2003), it was necessary to cross the Acadia Valley system in to the current study area. This proved difficult due to the extensive erosion in the valley system. In seismic section, it appears that both the flesh and carmine horizons were truncated by the overlying brown horizon. In stratigraphic order, the flesh and carmine horizons should lie between the rose and brown horizons respectively.

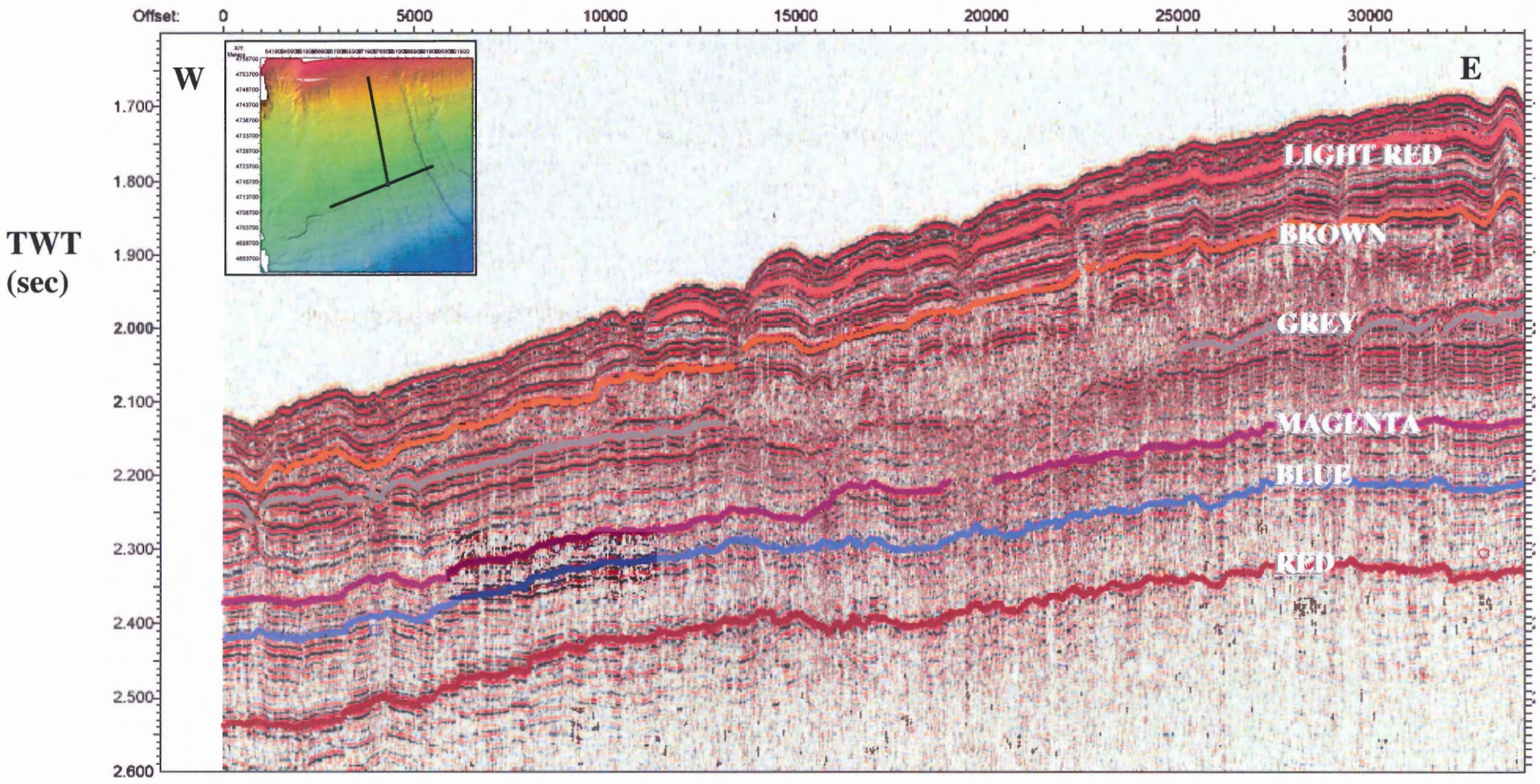

Fig. 3.4 – Regional strike line (CCGS Hudson Cruise 2004_030), illustrating the lateral seismic facies changes throughout the study area. Inset depicts location of this strike section as well as the following down-dip section.

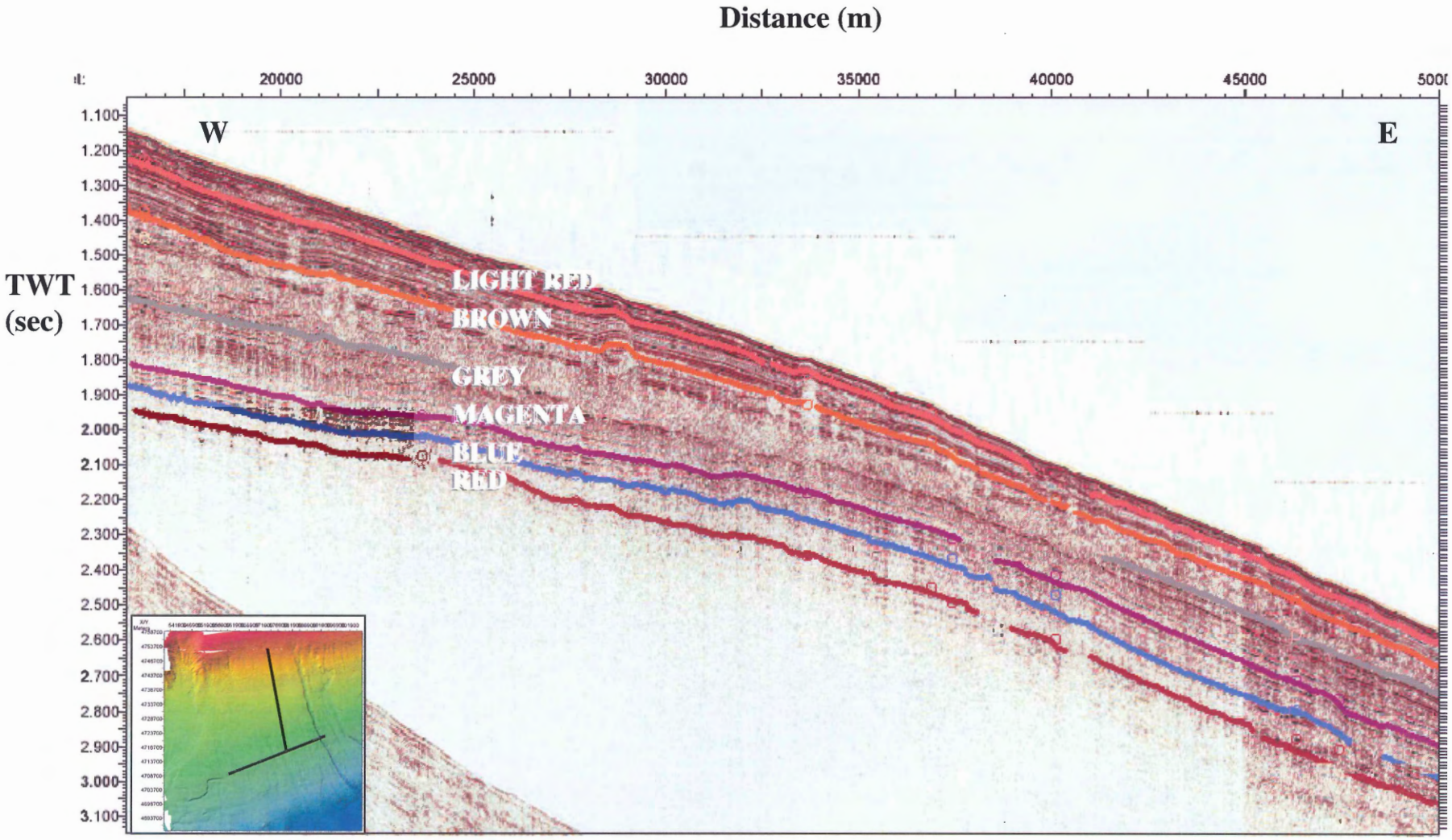

Fig. 3.5 – Regional down-dip line (CCGS Hudson Cruise 2004_030), illustrating the seismic facies changes down the slope throughout the study area. Inset illustrates both the location of this down-dip and the strike section.

3.5 Isochron Maps

Isochron maps illustrate the total thickness of a given temporal interval in two-way travel time (seconds). These maps do not provide sediment thickness in depth measurements (metres). However, the isochron is a function of the velocity profile of the geological material, and in the shallow section, velocities are not expected to vary greatly, therefore we can assume thickness relationships are approximately proportional. The maps offer valuable information regarding sedimentation processes.

Each stratigraphic interval that has been correlated within the study area has an associated isochron map. The base isochrons including red-blue and blue-magenta intervals exhibit no significant changes in thickness throughout the study area. In contrast, the grey-brown isochron clearly demonstrates thinning towards the southwest (Figure 3.6). The uppermost isochron corresponds to the brown-light red interval. This isochron has not been extended throughout the entire study area because the specific light red horizon was not resolved in certain surveys; therefore the isochron does not represent the thickness of the interval throughout the study area. However, in seismic section, the interval demonstrates notable downslope and westward thinning despite the absence of the light red key horizon.

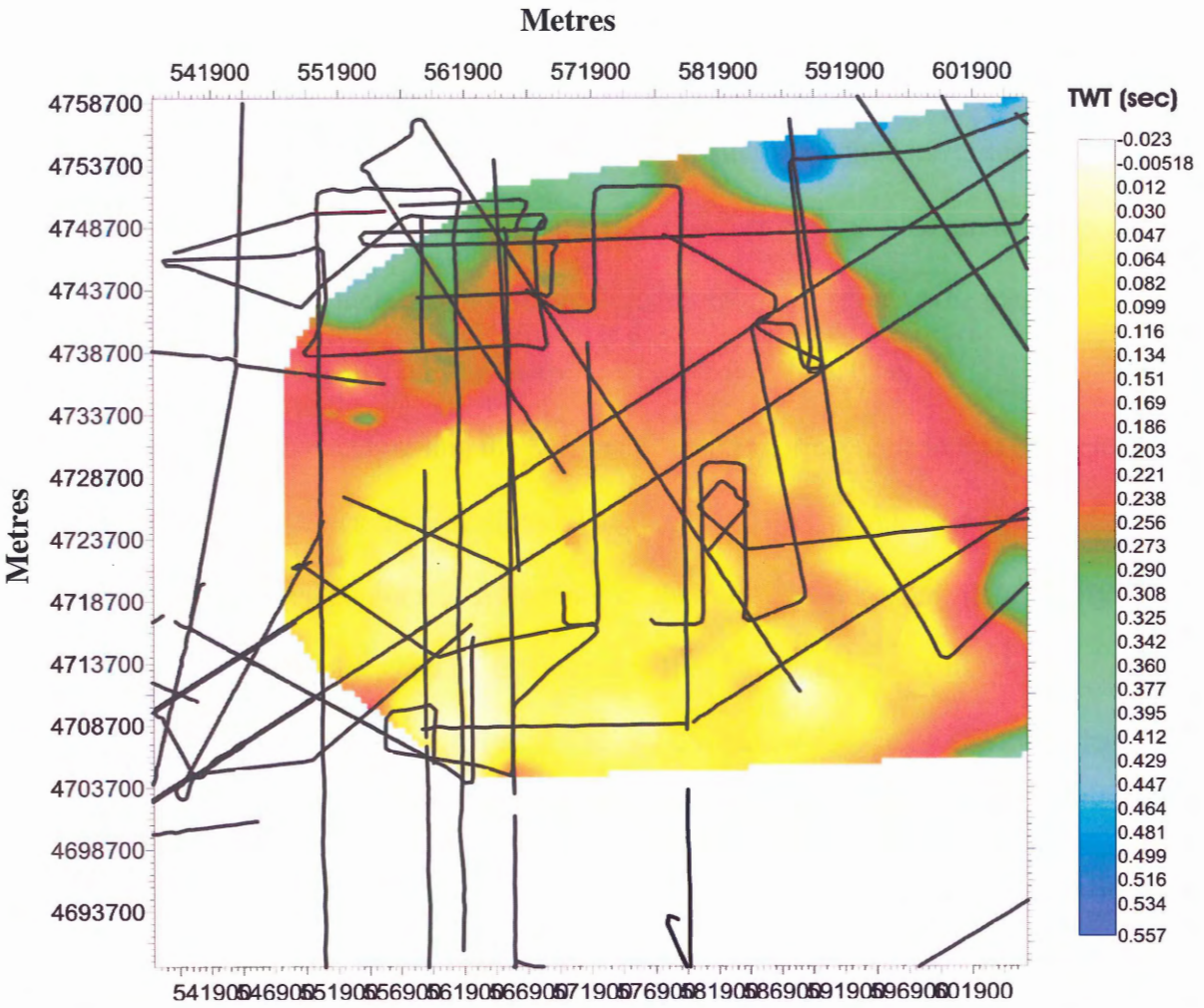

Fig. 3.6 – Isochron map of the grey-brown stratigraphic interval. The colour bar indicates the thickness of the interval with two-way travel time (TWT).

3.6 Mohican Channel

The Mohican Channel is a unique stratigraphic and morphological feature of the study area, encompassing several seismic stratigraphic intervals. The channel lies in the west of the study area and extends normal to the strike of the Scotian Slope. Survey lines 2002-046_15 and 2002-045_51 provide a seismic cross-section of the Mohican Channel at mid-upper slope that is illustrated in Figure 3.7. Survey line 2002-046_53 is a partial cross-section of the channel towards the base of the slope. Within all three seismic

sections, the channel incises the stratigraphy from the sea floor down to the grey horizon. Although there is significant loss in resolution beneath the channel itself due to signal attenuation, it is possible to interpret that basal reflectors red and blue are not affected by the overlying channel incision. It is difficult to interpret; however, if the magenta horizon is truncated by the channel incision without additional seismic data.

Acoustic character within the Mohican Channel corresponds to that of Facies C, with high amplitude chaotic reflections. The highly chaotic seismic character of the channel cuts parallel, continuous reflections of the surrounding seismic data clearly denoting the channel sides and base. Deeper in the channel at approximately 1.7 – 1.9 seconds the character changes to that of Facies D, with low amplitude chaotic reflections. This lowering of amplitude may be a result of vertical attenuation of the seismic signal; however, it is difficult to determine if this is the sole cause of the facies change without correlation to well data. Towards the base of the slope, portions of the channel show occurrences of Facies A. These parallel reflectors are noted close to the channel walls and are not present in the upper slope cross-section.

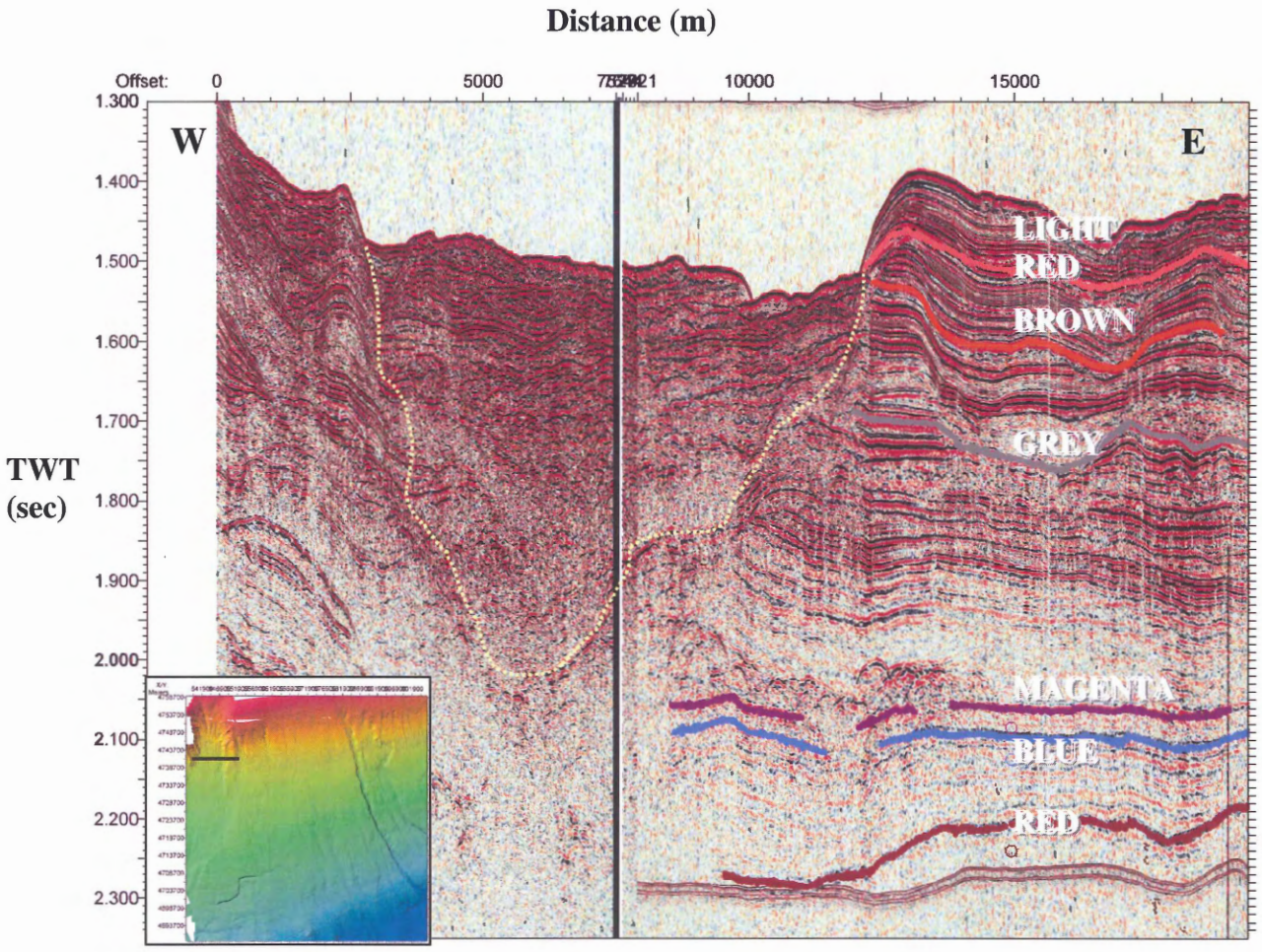

Figure 3.7 – Seismic cross-section of mid-upper slope Mohican Channel, survey lines 002-046_51 and 2002-046-15 respectively. Note: surveys do not match directly, and produce a minor gap in the seismic data; however, the missing section spans only ten's of meters. Dotted line represents channel incision. Inset depicts location of seismic line in the study area.

One down-dip section of the Mohican Channel is available from survey lines 2002-046_16 and 2002-046_50. Line 2002-046_16 is illustrated in Figure 3.8. No horizons have been correlated through these lines due to the highly variable seismic facies successions. Facies within this section are variably distributed, and primarily consist of Facies A, C, D and F. Specifically, a wedge of Facies D thins from the upper slope and pinches out at mid-lower slope levels. At a depth of approximately 200 ms below the seafloor, several continuous reflections are truncated at an oblique channel

shaped feature, likely representative of a small side gully of the Mohican Channel. At mid-slope, the seafloor exhibits a smooth step-like character, down dip of which multiple occurrences of Facies D are dispersed.

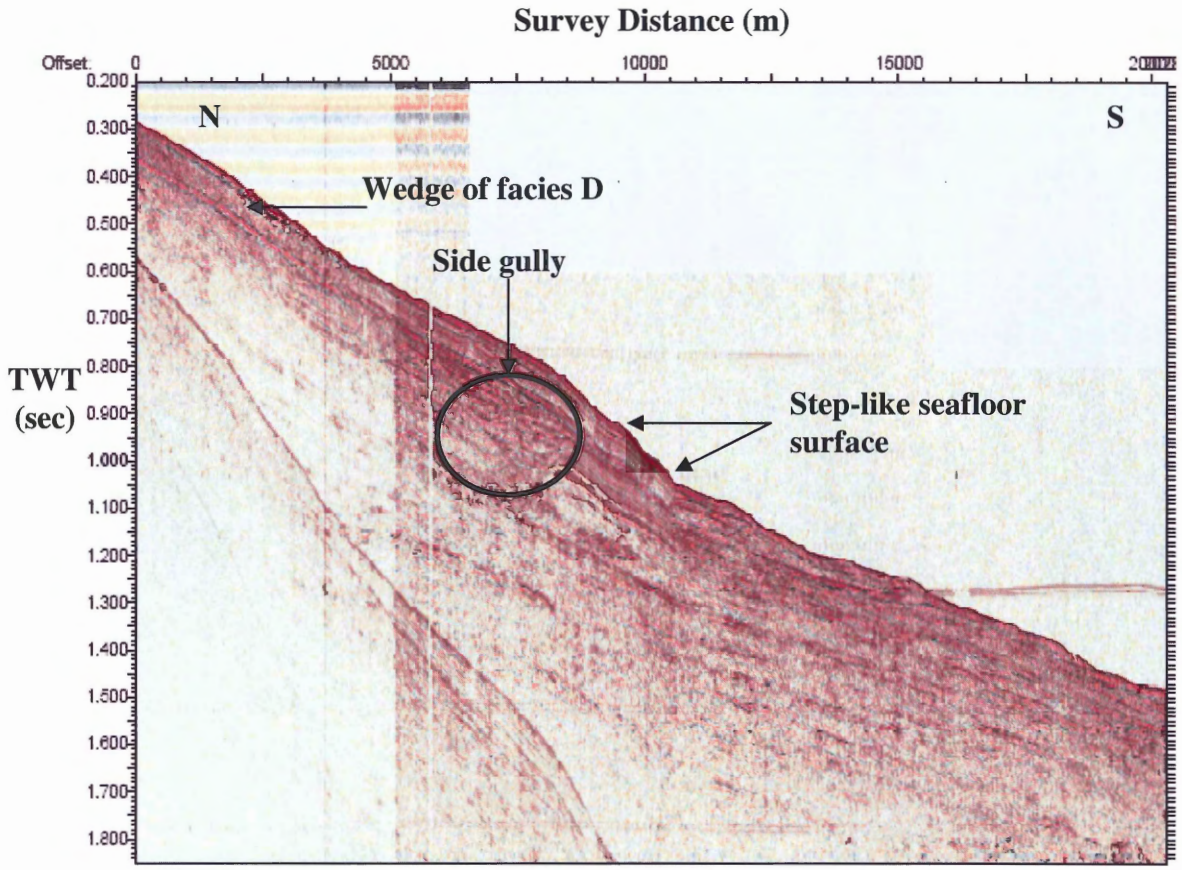

Fig. 3.8 – Survey line 2002-046_16, mid-upper slope seismic section of the Mohican Channel.

3. 7 Faults

Within the red-blue and blue-magenta intervals, faulting is present at a regional scale (Newton 2003). Figure 3.9 displays an example of this widespread faulting on survey 2004030_line14b. Both the red and blue horizons are visibly offset by this faulting. It is difficult to determine whether the magenta horizon is offset by the faulting or whether the reflections drape the underlying topography created by the faults. The faults are near vertical and primarily show normal offset both in strike and down-dip section.

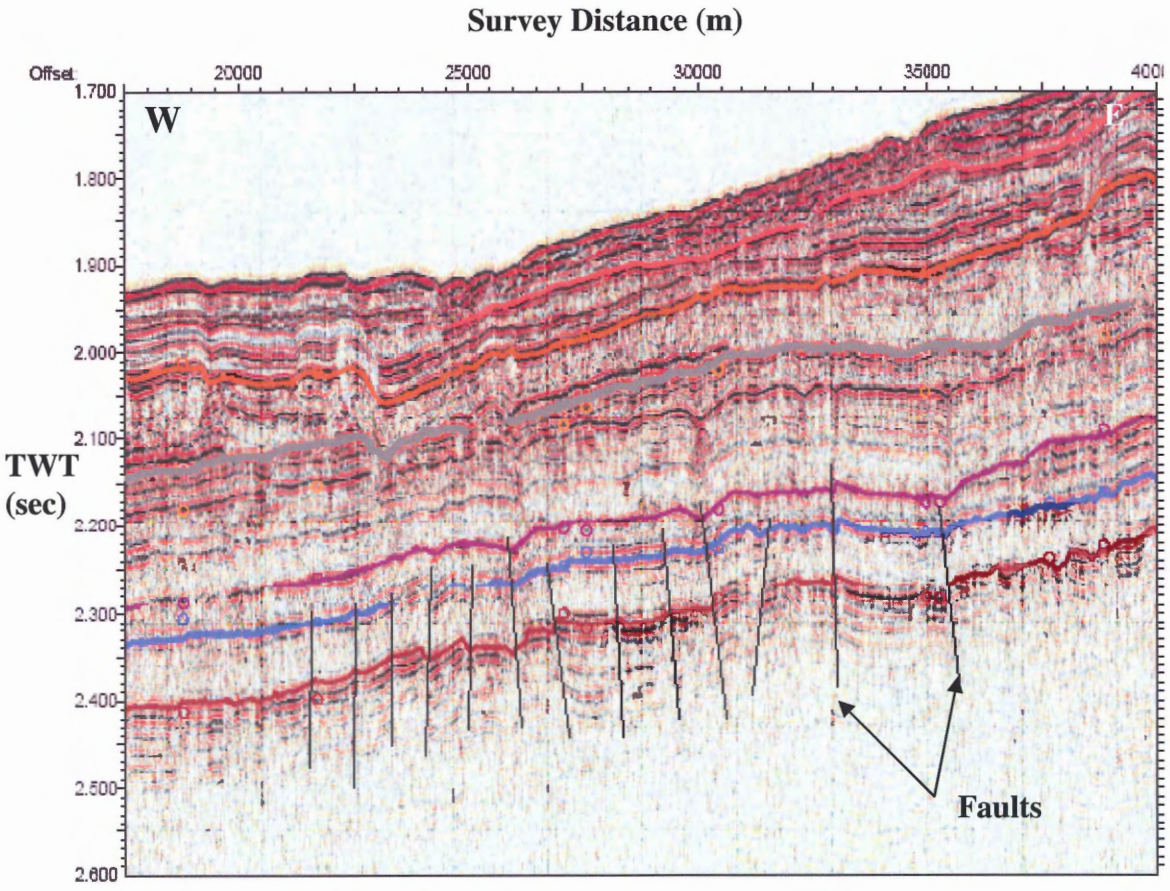

Figure 3.9 – Illustration of faulting within red-blue and blue-magenta intervals on line 2004030_line14b. Faults are represented by black lines.

3.8 Digital Deep-towed Hydrophone data

Survey line 2002-046_53DDH provides the best example of a fully processed DDH seismic section and is illustrated in Figure 3.10. For comparison, Figure 3.11 is an example of the corresponding conventional reflection seismic section that was acquired simultaneously. The processed DDH section demonstrates excellent resolution in the upper strata as predicted. Seismic facies in the DDH data, specifically in the upper 100 ms, are more defined than in the conventional seismic data. However, seismic definition is lost rapidly with depth and several deep horizons are difficult to identify in comparison to the conventional section. This result is likely due to the comparably shorter hydrophone streamer used as a receiver for the DDH survey. The frequency that a receiver can detect is a function of the length of the streamer and spacing of the hydrophones. Low frequencies that can penetrate deepest are lost as the receiver is shortened because the wavelength of the lower frequency signals is longer and is insufficiently sampled by a short streamer. Additionally, on a shorter streamer there are fewer hydrophone channels to sum. Therefore, the few low frequency signals cannot be separated as effectively from the background noise. Under-sampling of low frequencies results from the effect of a short streamer.

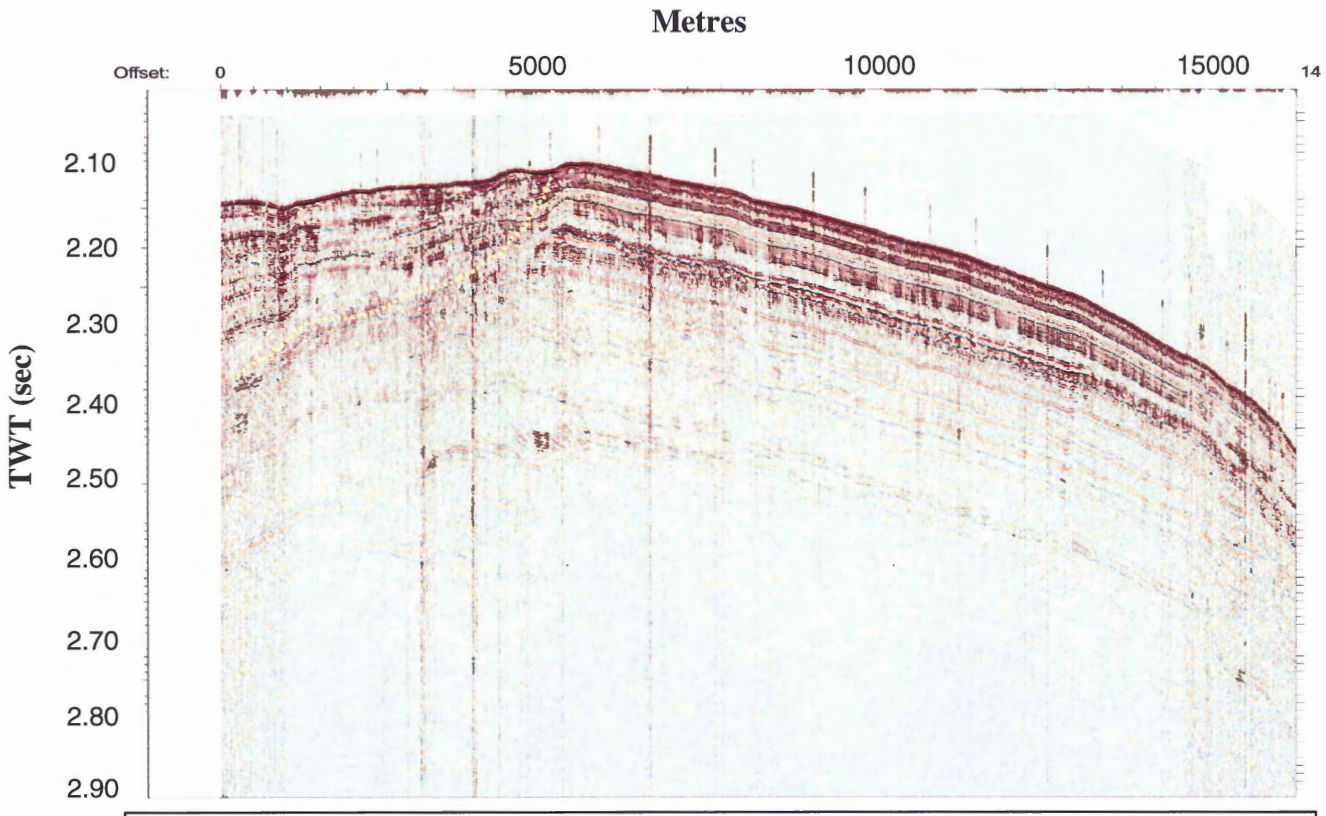

Figure 3.10– Example of a processed DDH section, survey line 2002-046_53DDH.

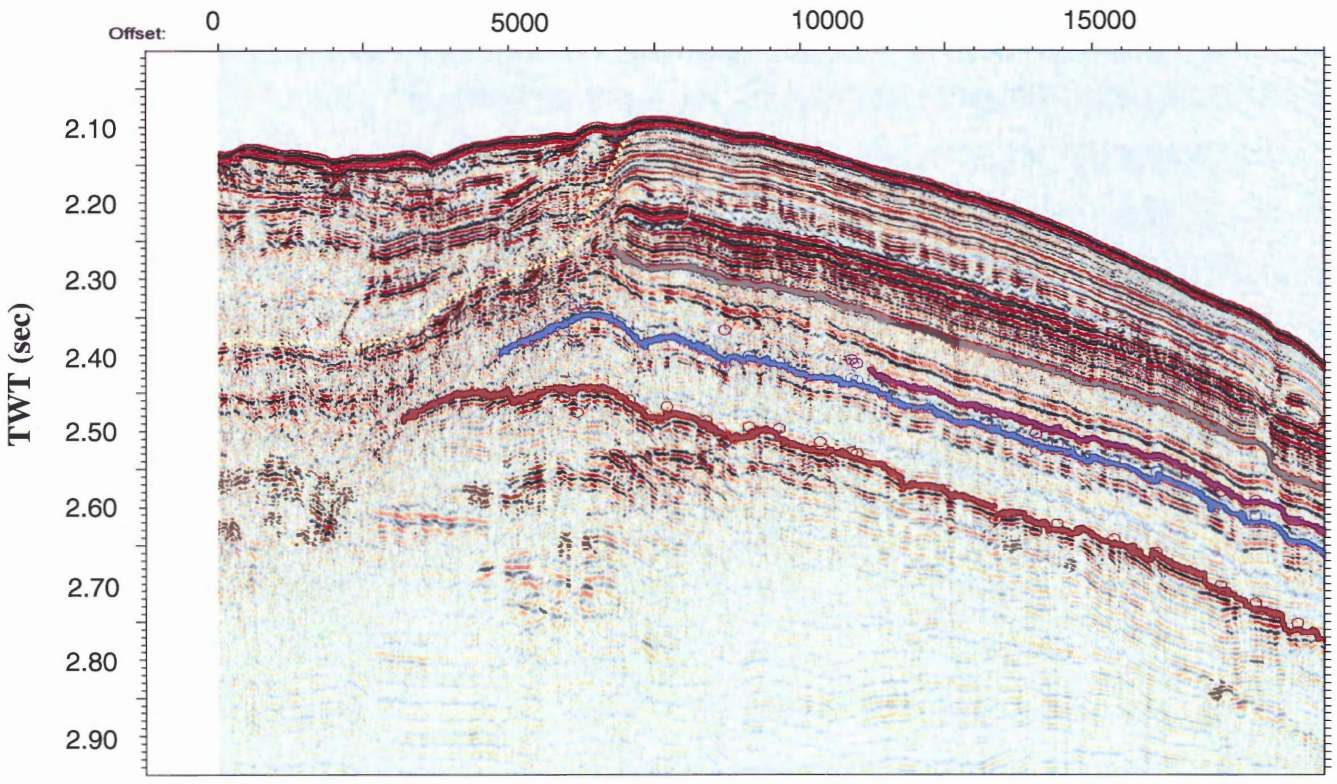

Figure 3.11– Example of a processed conventional 2D reflection seismic section, survey line 2002-046_53_teledyne. Dotted line shows western base of the Mohican Channel

CHAPTER 4

DISCUSSION AND CONCLUSIONS

4.1 Assessment of DDH Technique

Processing techniques for digital deep-towed hydrophone (DDH) data were developed on Line53 of Hudson Cruise 2002-046, which lies in the southwest quadrant of the study area. Corresponding conventional 2D seismic data for the same line are available for comparison of the two acquisition techniques. Line53 is the only processed DDH seismic section within the study area.

Successful reconstruction and processing of DDH data resulted in vertical resolution of about 0.5 – 1 m, while comparable conventional surface-towed data resolution is about 2 m. Maximum resolution is calculated as one quarter the wavelength of the seismic signal. The dominant frequency of conventional seismic data is approximately 180 Hz whereas that of DDH data is notably higher at 350-400 Hz. Unfortunately, DDH seismic data below about 200 ms were attenuated in comparison to conventional reflection seismic data because of the short hydrophone streamer used in the DDH configuration. The short array is necessary to control the geometry of the array at slow tow speeds and to submerge the deep streamer and acquisition package to great depths.

DDH data have proven to be ineffective in establishing the seismic stratigraphy within this project area because of the short imaging depth and the scarcity of data. For the purposes of this study conventional reflection seismic data are utilized for geological interpretation. However, the successful processing and higher shallow resolution of the DDH data show that the technique has potential for future studies, particularly in areas of

complex physiography. Further refinement of the acquisition and processing methods will result in a new tool for seismic stratigraphic analysis.

4.2 Stratigraphy and Age Constraints

Biostratigraphic control of the late Cenozoic seismic stratigraphy is provided by the Acadia K-62 and Shubenacadie H-100 wells. Piper and Sparkes (1990) used these data to provide approximate ages for key horizons that were correlated to the study area (Table 1.1). From the Shubenacadie H-100 well, samples that relate to the red horizon are denoted as mid-Late Pliocene age. The red horizon is the deepest resolved horizon of the seismic data, therefore biostratigraphic control beneath this horizon is not considered within this study. From the Acadia K-62 well, the grey horizon corresponds to the interpreted base of the Quaternary period based on known foraminiferal assemblages observed in well cuttings. Finally, the carmine horizon of Piper and Sparkes (1990) is defined as marking the first shelf-crossing glaciation that occurred on the Scotian margin (Piper, 2001). Although this horizon was not successfully correlated to the study area, its stratigraphic position occurs between the grey and brown horizons. This event has been estimated at an age of 0.45 Ma (Piper, 2001) and denotes the interpreted transition between non-glacial and glacial deposition on the Scotian Slope.

Seismic data used in this investigation encompass sediments from mid-Late Pliocene to Holocene in age. Figure 4.1 illustrates the age distribution within a seismic type-section, as interpreted from known biostratigraphic control (Piper and Sparkes, 1990). As seen in this figure, the Late Pliocene and Pleistocene comprise the majority of the section. Only a thin veneer of Holocene sediments are resolved in the upper

reflections of these data. The mid-Late Pliocene encompasses horizons red through grey, the Pleistocene encompasses horizons brown and light red, and finally the Holocene encompasses only the topmost seismic reflections, to which no key horizon has been ascribed.

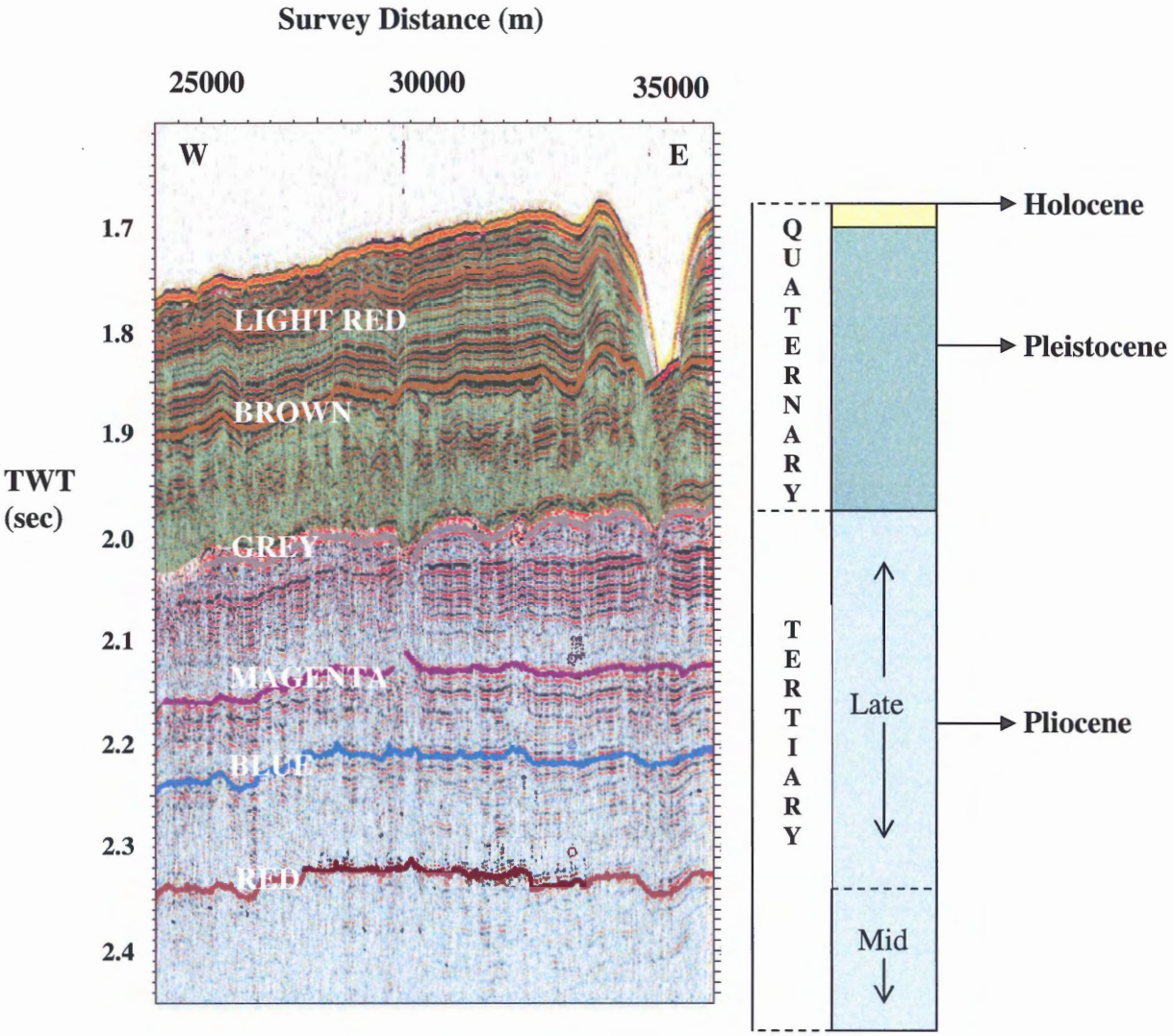

Fig. 4.1 – Age control of the seismic stratigraphy, based on data from Piper et al. (1987)

4.3 Synthesis of Depositional Environments

Seismic facies analysis is the interpretation of the characteristics of a rock or sediment interval based on its acoustic reflection properties in seismic data. The configuration, continuity and amplitudes of reflections within a seismic facies are interpreted for lithology and depositional processes. While the configuration and continuity of reflections indicate bedding patterns and depositional processes, the reflection amplitude reveals properties such as impedance, grain size, bed spacing and fluid content (Hart, 2000). Six seismic facies observed within the study area represent different sedimentation processes that were active within the Late Pliocene and Quaternary; their interpretation is based on the presumed depositional environment and association with other seismic facies.

Deposition on the Scotian Slope can be subdivided into two major groups: 1) dominated by non-glacial deposition and 2) dominated by glacial deposition. The major shelf-crossing glaciation marker lies between the grey and brown horizons at a mid-Pleistocene age, and is approximated just below the brown horizon (Figure 3.3). The stratigraphy from the red horizon to mid-way above the grey horizon has experienced no direct influence from glaciation (Pliocene – mid-Pleistocene), whereas stratigraphy immediately below the brown horizon to the seafloor is glacially influenced (mid-late Pleistocene). Seismic facies within these intervals are interpreted in the context of their respective depositional environments: non-glacial and glacial deposition.

4.3.1 Non-glacial Deposition

Sedimentation Processes

The base of the non-glacial stratigraphy is characterised by alternating cycles of Facies A and B. This seismic facies pattern is interpreted as cycles of deposition dominated by turbidity currents and those dominated by hemipelagic sedimentation.

Facies A consists of high amplitude, continuous and parallel reflections that are indicative of unconfined turbidity current deposition (Mosher et al., 1994). Characteristically, this process is widespread on the slope, creating continuity in seismic reflections. The high amplitudes of the facies likely represent the impedance between the fine-grained fraction and sand fractions of the turbidite sequence. Turbidity currents are either confined within canyons and channels, or unconfined and spread laterally over the slope (Mosher et al., 2004). Unconfined, low density turbidity currents are interpreted within the study area because the reflections are correlatable laterally over large distances. They are attributed to periods of significant off-shelf sediment transport. These bursts of sediment influx probably resulted from storm currents that reached the edge of the continental shelf during Late Tertiary sea-level lowstands (Mosher et al., 2004).

Facies B represents low amplitude, continuous and parallel reflections that are interpreted as hemipelagic background sedimentation. Continuity of reflections results from the uniform draping of this sedimentation process and the low reflection amplitude probably indicates fine grain size and little acoustic impedance between beds. Piper et al. (1990) suggested that sequences with these characteristics occur during non- and

interglacial periods that would represent sea-level highstands and are associated with relative slope stability.

At mid-level within the non-glacial section, Facies E appears just below the grey horizon. The hummocky reflections of this facies represent gullies and gully overspill creating channel levee morphology. This facies characteristic marks the base of the Pleistocene (grey horizon), at which point gullies were widespread on the slope in response to a significant sea-level lowstand (Kidston et al., 2002).

A large unit of Facies D is present in the upper non-glacial stratigraphy and lies directly over the grey horizon. Low amplitude, chaotic reflections in seismic data on the Scotian Slope are interpreted by Mosher et al. (2004) to represent mass transport deposits (MTD). The incoherent reflection configuration is attributed to reworking and re-deposition of slope material and the low amplitude is a result of low impedance due to homogenous mixing.

The MTD truncates the underlying grey (basal Pleistocene) horizon in several areas indicating an early Pleistocene age. The deposit is widely correlatable throughout the study area, spans a lateral distance of roughly 30 km, and encompasses a downslope distance of at least 20 km. Simpson (2005) interpreted and rendered the MTD surface using 3D seismic data within the area (Figure 4.2). Large debris blocks depicted within the MTD surface measure up to 500 m in size indicating that material was transported under unstable slope conditions. These same blocks exhibit strong north-south alignments with shallow surficial linear channels, which suggest movement was primarily downslope. Simpson (2005) has also generated a 3D horizon of the base of the MTD that

supports the interpretation of downslope movement. Parallel striations aligned down-dip indicate scouring of the underlying material as the unit was deposited.

Based on the definition of Canals et al. (2004), this MTD can be classified as a debris flow. A debris flow is defined as a mass movement of varying kinds of debris; particularly high density mud that contains entrained coarse grained material. The flow in this study appears to primarily consist of fine grained material, manifest in the smooth areas of the surface, which supports a significant content of coarse blocky material as observed in the Figure 4.2.

Non-Glacial Mass Failure Trigger Mechanisms

Non-glacial trigger mechanisms considered for high-latitude continental margins such as the Scotian margin include: 1) earthquakes, 2) oversteepening and faulting on the slope initiated by salt tectonics, 3) slope oversteepening through erosion, 4) off-shelf sediment transport from storm currents 5) dissociation of gas hydrates and 6) gas escape from underlying reservoirs (Mosher et al., 2004). To trigger such a large scale failure, as shown above, the most probable mechanism is a combination of some of these events. Canals et al. (2004) suggest that pre-conditioning processes such as erosion, off-shelf transport, and gas escape require a final large-scale trigger such as an earthquake to produce sufficient slope instability. This hypothesis is reasonable to apply to the debris flow within the study area because it is an uncommon feature suggesting a low recurrence interval, characteristic of passive margin seismicity.

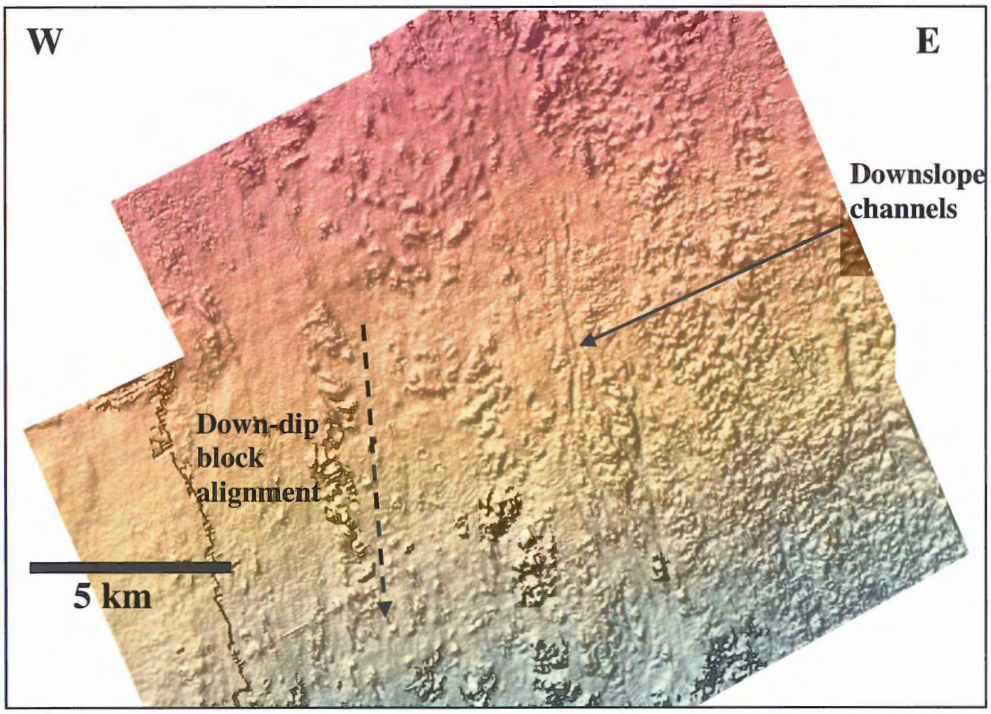

Fig. 4.2 – 3D render of the large debris flow surface within the study area (Simpson, 2005).

4.3.2 Glacial deposition

Sedimentation Processes

Cycles of Facies A and B are thinner and more frequent in the glacial stratigraphy than the deeper, non-glacial section. Major sedimentation processes represented by the seismic facies are again low density turbidity current deposition and hemipelagic drape, respectively.

Origin of the material transported by turbidity currents is different during glacial periods than that of non-glacial periods. Sea levels are characteristically low during glaciations and therefore, the frequency of unconfined turbidity currents is significantly higher throughout glacial stages as a result of the higher influx of outwash material

during stages of ice retreat. The glacial outwash in close proximity to the shelf break initiates fluxes of low density turbidity currents during these glacial periods.

Hemipelagic sedimentation, represented by Facies B, likely dominated during the sea level highstands of interglacial stages of the mid-Late Pleistocene. This process probably did not vary significantly from that of non-glacial periods.

Facies F is present in the upper section of the glacial interval and has been interpreted to represent several possible sedimentation processes. The interbedded chaotic reflections likely represent two glacial processes: 1) local deposition of ice-rafted debris and 2) deposition of thin failure deposits associated with ice retreat. The high amplitude parallel reflections, that are also present in the facies, are representative of continued interaction of turbidity current deposition throughout the late glacial stage. The late Pleistocene occurrence of Facies F suggests periods of slope instability.

Glacial Mass-Failure Trigger Mechanisms

The trigger mechanisms proposed for slope instability during glacial deposition vary from those of non-glacial periods; they include 1) glacial loading / unloading resulting in isostatic adjustment and possible seismicity, 2) glacial loading resulting in salt deformation and subsequent slope oversteepening, 3) ice loading at the shelf break inducing vertical stress, 4) lithostatic loading resulting from influx of proglacial sediment, and 5) turbidity flows eroding and oversteepening the slope (Mosher et al., 2004). A combination of several of these factors is probably responsible for triggering mass-failures during glacial epochs.

4.3.3 Mohican Channel

The Mohican Channel notably incises the Pleistocene stratigraphy from the seafloor to a depth of at least the grey horizon, which indicates that it was active throughout the last Pleistocene glaciation. Facies C, the principal seismic facies identified within the channel, indicates that the primary sedimentation process has been high energy glacial outflow. The high amplitude, chaotic reflections of the facies possibly represent reworked material, deposited during glacial stages. Consequently, the channel has been interpreted as a major glacial outwash conduit of the late Pleistocene.

Levee deposits at the banks of the Mohican Channel are open to interpretation; and are not obvious in the seismic data. Without preserved levee or overbank deposits to indicate previous periods of channel activity, it is not possible to indicate its maximum age.

Rare occurrences of Facies A indicate that episodic high energy deposition may have been interrupted by periods of slow, uniform accumulation during interglacial highstands. Failure scarps are observed in down-dip seismic section in the morphology of the seafloor (Figure 3.8). The proximity of these features to the seafloor is indicative of channel activity within the last glacial advance on the Scotian margin.

The study area exhibits a uniquely smooth surficial morphology between the Acadia Valley system to the east and the Mohican Channel to the west. The smooth slope surface may be explained by a distal ice margin, which did not extend completely to the shelf edge at this site. Consequently, the Mohican Channel may have transported sediment from a greater distance than other channels on the eastern slope. The absence of till tongues in seismic section within the study area is further support of a distal ice

margin. Till tongues are wedge-shaped, incoherent depositional products of the ice sheet grounding on the shelf edge (King and Fader, 1985; Gauley, 2001) and have not been resolved within the seismic data of the study area.

Table 4.1 – Summary of the late Cenozoic depositional history within the study area

Depositional Environment	**Age**	**Sedimentation Processes**	**Facies Representation**
Non-glacial	Pliocene to mid-Pleistocene (~3 Ma – 0.45 Ma)	- turbidite deposition - hemipelagic - MTD - widedspread gullying	Facies A Facies B Facies D Facies E
Glacial	mid-late Pleistocene (0.45 Ma – 16,000 BP)	- turbidite deposition - hemipelagic - channel outflow - ice-rafting and thin mass failure	Facies A Facies B Facies C Facies F
Post-glacial	late Pleistocene – Holocene (16,000 BP – Recent)	- hemipelagic	* from Mosher et al., 2004, Pickrill et al., 2001.

4.4 Faulting

A prominent feature observed during the correlation of horizons was the extensive faulting constrained between the red-blue and blue-magenta stratigraphic intervals (Figure 3.9). The faults are apparent both in strike and down-dip seismic section and they are observed extensively throughout the study area. Regional studies on the Scotian Slope have described a polygonal geometry to the fault systems (Hansen et al., 2004), that may be similar in genesis to the fault pattern observed in this study.

Widespread polygonal faulting in Cenozoic sediments is observed in numerous sedimentary basins worldwide (Dewhurst et al., 1999). Various hypotheses have been presented to explain the presence of this polygonal fault system. Dewhurst et al. (1999) and Hansen et al. (2004) attribute the formation of these structures to syneresis in the sedimentary layers. Syneresis is the process of three dimensional contractions of sedimentary gel-like material and associated dewatering. The resulting polygonal fault geometry, analogous to common mudcracks, is not attributed to gravity-driven mechanisms (Dewhurst et al, 1999).

An additional mechanism proposed for the genesis of the faults and their complex pattern indicates that these structures are formed as a result of large-scale deformation creep. Creep is a gravity driven process involving slow, downslope deformation (extension) in a stratigraphically confined interval, involving a decollement at the lower and possibly upper surface. A model suggested by Goulty (2001) indicates that differential stresses resulting from passive subsidence may be responsible for the initiation and growth of the fault pattern. However, general agreement on the origin of these polygonal fault systems does not exist and was beyond the scope of this study

4.5 Conclusions

1) The late Cenozoic Scotian Slope has experienced both non-glacial and glacial deposition. Non-glacial deposition encompasses the Pliocene to mid-Pleistocene section, in which hemipelagic sedimentation, turbidity current deposition and mass transport deposits prevailed. Glacial deposition occurred throughout the mid-late

Pleistocene and included hemipelagic sedimentation, turbidity current deposition, small-scale mass failure and localized ice-rafting.

2) Trigger mechanisms for slope failure differ between non-glacial and glacial environments. Non-glacial mechanisms include earthquakes, slope oversteepening by erosion or salt tectonics, off-shelf transport via storm currents, and dissociation of gas hydrates. The mechanism interpreted as most likely to cause the major debris flow within the non-glacial period is passive margin seismicity. Glacial trigger mechanisms additionally include seismicity from glacial loading and unloading, lithostatic loading from influx of proglacial sediment, oversteepening of the slope by turbidity currents, and dissociation of gas hydrates due to bottom water temperature changes. A combination of these mechanisms is the likely trigger for glacial failures.

3) The digital deep-towed hydrophone acquisition technique successfully resolved the upper strata of the study area; however, due to signal attenuation in the lower strata and lack of trials within the study area, it was not applied to the seismic stratigraphic analysis of the study area. These data, however, demonstrate potential for use in further studies, particularly in areas of steep or rugged terrain and where fine resolution is required in the topmost of sediments.

4.6 Implications for Offshore Development

Development in the deep-water offshore Nova Scotia necessitates the study of surficial and Cenozoic geology to mitigate the risks of slope failure and its effects on seafloor infrastructures. Under present day conditions, deposition on the Scotian Slope is dominated by hemipelagic background sedimentation. Consequently, the slope is stable

and likely requires a triggering mechanism to initiate failure over most of the slope (Mosher et al., 1994). This study indicates passive margin seismicity as a likely trigger mechanism for failure during periods of non-glacial deposition. The recurrence interval of earthquakes on this passive margin is not well-known, but is expected to be on the order of tens to hundreds of thousands of years.

4.7 Recommendations for Future Work

There is much opportunity for further studies in Plio-Pleistocene deposition on the central Scotian Slope. Future work from this study can be divided into 1) refinement of the DDH acquisition technique and 2) further analysis of the late Cenozoic seismic stratigraphy.

Both acquisition and processing techniques for DDH data can be improved for better application to seismic stratigraphic interpretation. Additional trial surveys would be beneficial; specifically in regions with well-studied seismic stratigraphy for comparison. Use of a longer hydrophone streamer may result in resolution of deeper seismic reflections and would further enhance the quality of the DDH data. This study has demonstrated that it is a promising technique that, with improvement, will be a valuable tool for seismic investigations.

Ground-truthing with lithologic and biostratigraphic information will be beneficial to the interpretation of seismic facies and refinement of age control. Currently, limited core data are available in the late Cenozoic section but additional information from the academic community and industry partners will develop the understanding of slope processes significantly. Additional study of the relationship of the Mohican

Channel to the surrounding stratigraphy may better constrain its age and dynamics. This study contained limited surveys across the channel and due to time constraints an in-depth analysis was not completed; however, it is an interesting morphological feature that is worth studying in greater detail.

REFERENCES

Campbell, D.C., Shimeld, J.W., Mosher, D.C., Piper, D.J.W. 2004. Relationships between sediment mass-failure modes and magnitudes in the evolution of the Scotian Slope, offshore Nova Scotia. Offshore Technology Conference. 16743. Houston. 13 pp.

Canals, M., Lastras, G., Urgeles, R., Casamor, J.L., Mienert, J., Cattaneo, A., De Batist, M., Haflidason, H., Imbo, Y., Laberg, J.S., Locat, J., Long, D., Longva, O., Masson, D.G., Sultan, N., Trincardi, F., Bryn, P. 2004. Slope failure dynamics and impacts from seafloor and shallow sub-seafloor geophysical data: case studies from the COSTA project: Marine Geology, **213:** 9-72.

Dewhurst, D.N., Cartwright, J.A., Lonergan, L. 1999. The development of polygonal fault systems by syneresis of colloidal sediments. Marine and Petroleum Geology, **16**: 793-810.

Emery, K.O., Uchupi, E. 1984. The Geology of the Atlantic Ocean. Springer-Verlag. New York. p. 44-102.

Gauley, B.-J.L. 2001. Lithostratigraphy and sediment failure on the central Scotian Slope. M.Sc. thesis, Dalhousie University, Halifax, Nova Scotia, 214 pp.

Goulty, N.R. 2001. Polygonal fault networks in fine-grained sediments – an alternative to the syneresis mechanism. First Break, **19**: 69-73.

Hansen, D.M., Shimeld, J.W., Williamson, M.A., Lykke-Andersen, H. 2004. Development of a major polygonal fault system in Upper Cretaceous chalk and Cenozoic mudrocks of the Sable Subbasin, Canadian Atlantic Margin. Marine and Petroleum Geology, **21**: 1205-1219.

Hart, Bruce. 2000. 3-D Seismic Interpretation: A Primer for Geologists. Society for Sedimentary Geology Short Course No. 48. Tulsa. p 47-56.

Keen, C.E. Loncarevic, B.D., Reid, I., Woodside, J., Haworth, R.T., Williams, H. 1990. Tectonic and geophysical overview. *In* Geology of the continental margin of eastern Canada. *Edited by* M.J. Keen and G.L. Williams. Geological Survey of Canada Geology of Canada No. 2, Chap. 2, p. 31-85.

Kidston, A.G., Brown, D.E., Altheim, B., and Smith, B.M. 2002. Hydrocarbon Potential of the Deep-Water Scotian Slope. Canada-Nova Scotia Offshore Petroleum Board, Halifax, Nova Scotia, 111 pp.

King, L.H., and Fader, G.B. 1986. Wisconsinan Glaciation on the continental shelf – southeast Atlantic Canada. Geological Survey of Canada, Bulletin 363.

LeBlanc, R.C. 2002. Central Scotian Slope stability: the possible role of methane hydrates. Unpublished B.Sc. (honours) thesis, Dalhousie University, Halifax, Nova Scotia, 79 pp.

Louden, Keith. 2002. Tectonic Evolution of the East Coast of Canada. CSEG Recorder. p. 37-48

MacDonald, Fiona. 2003. Glacial Geology and Geochronology of Peggy's Cove Region. B.Sc. thesis, Dalhousie University, Halifax, Nova Scotia, 77 pp.

Mosher, D.C. 1987. Late Quaternary sedimentology and sediment instability of a small area on the Scotian Slope. M.Sc. thesis, Memorial University of Newfoundland, St. John's, Newfoundland, 248 pp.

Mosher, D.C. 2000. CCGS Hudson Cruise 2000-042 expedition report, Scotian Slope. Unpublished GSC Internal Report, 50 pp.

Mosher, D.C. 2001. CCGS Hudson Cruise 2001-048A expedition report, Scotian Slope. Unpublished GSC Internal Report, 50 pp.

Mosher, D.C. 2005. CCGS Hudson Cruise 2004-030 expedition report, Scotian Slope. Unpublished GSC Report. 73 pp.

Mosher, D.C., Moran, K., Hiscott, R.N. 1994. Late Quaternary sediment, sediment mass-flow processes and slope stability on the Scotian Slope. Sedimentology, **41**: 1039-1061.

Mosher, D.C., Piper, D.J.W., Campbell, D.C., Jenner, K.A. 2004. Near-surface geology and sediment-failure geohazards of the central Scotian Slope: American Association of Petroleum Geologists bulletin, **88**: 703-723.

Newton, C.S. 2003. Quaternary and Late Pliocene Seismic Stratigraphy of the Central Scotian Slope. B.Sc. thesis, Dalhousie University, Halifax, Nova Scotia, 108 pp.

Pickering, K.T., Hiscott, R.N., Hein, F.J. 1989. Deep-marine environments: clastic sedimentation and tectonics. Unwin Hyman. London. 416 pp.

Pickrill, R., Piper, D.J.W., Collins, J., Kleiner, A., Gee, L. 2001. Scotian Slope Mapping Project: The benefits of an integrated regional high-resolution multibeam survey.

Piper, D.J.W. 1999. CCGS Hudson 1999-036 expedition report, Scotian Slope. Unpublished Internal GSC Report, 86 pp.

Piper, D.J.W. 2001. The Geological Framework of Sediment Instability on the Scotian Slope: Studies to 1999. Geological Survey of Canada Open file 3920, 202 pp.

Piper, D.J.W., and Mosher, D.C. 2002. CCGS Hudson Cruise 2002-046 expedition report, Scotian Slope. Unpublished GSC Internal Report, 62 pp.

Piper, D.J.W. and Sparkes, R., 1990. Pliocene – Quaternary geology, central Scotian Slope. Geological Survey of Canada Open File 2233.

Piper, D.J.W., Normark, W.R. and Sparkes R. 1987. Late Cenozoic acoustic stratigraphy of the central Scotian Slope, eastern Canada: Canadian Bulletin of Petroleum Geology, **35**: 1-11.

Piper, D.J.W., Mudie, P.J., Fader, G.B., Josenhans, H.W., MacLean, B., and Vilks, G. 1990. Quaternary Geology. In Geology of the continental margin of eastern Canada. Edited by M.J. Keen and G.L. Williams. Geological Survey of Canada Geology of Canada No.2, Chap. 10, pp. 475-607.

Reading, H.G. 1986. Sedimentary Environments and Facies. 2nd ed. Blackwell Scientific Publications. Oxford. pp. 4 -19.

Shackleton, N.J. and Pisias, N.G., 1985. Atmospheric carbon dioxide, orbital forcing, and climate in: E.T Sundquist and W.S. Broeker (Eds.) The Carbon cycle and atmospheric CO2: natural variations Archean to present. Geophysical Monograph **32:** 412-417

Simpson, Kent. 2005. Cenozoic Sedimentation Processes of the Central Scotian Slope. Abstract. American Association of Petroleum Geologists. *In Press*.

Wade, J. and MacLean, B. 1990. The geology of the southern margin of Canada. *In* Geology of the continental margin of eastern Canada. *Edited* by M.J. Keen and G.L. Williams. Geological Survey of Canada Geology of Canada No. 2, Chap. 5, 167-238.